Advanced Membranes 3 (2023) 100070

Contents lists available at ScienceDirect

Advanced Membranes

journal homepage: www.keaipublishing.com/en/journals/advanced-membranes

Catalytic membrane reactors for carbon peaking and carbon neutrality

Jiuxuan Zhang [a,1], Bo Liu [a,1], Lili Cai [b,1], Yanhong Li [c], Yan Zhang [d,1], Mengke Liu [d], Lujian Jia [d], Senqing Fan [e], Linfeng Lei [f], Minghui Zhu [f], Xuefeng Zhu [b,g,**], Xuebin Ke [h], Aisheng Huang [c,***], Heqing Jiang [d,****], Rizhi Chen [a,*]

[a] State Key Laboratory of Materials-Oriented Chemical Engineering, Nanjing Tech University, Nanjing, 211816, China
[b] State Key Laboratory of Catalysis, Dalian Institute of Chemical Physics, Chinese Academy of Sciences, 457 Zhongshan Road, Dalian, 116023, China
[c] State Key Laboratory of Molecular & Process Engineering, Shanghai Key Laboratory of Green Chemistry and Chemical Processes, School of Chemistry and Molecular Engineering, East China Normal University, Dongchuan Road 500, Shanghai, 200241, China
[d] Qingdao Key Laboratory of Functional Membrane Material and Membrane Technology, Qingdao Institute of Bioenergy and Bioprocess Technology, Chinese Academy of Sciences, No. 189 Songling Road, Qingdao, 266101, China
[e] School of Chemical Engineering, Sichuan University, No. 24 South Section 1, Yihuan Road, Chengdu, 610065, China
[f] State Key Laboratory of Chemical Engineering, School of Chemical Engineering, East China University of Science and Technology, Shanghai, 200237, China
[g] University of Chinese Academy of Sciences, Beijing, 100049, China
[h] University of Hull, HU6 7RX, United Kingdom

ARTICLE INFO

Keywords:
Catalytic membrane reactor
Catalytic membrane
Carbon peaking
Carbon neutrality

ABSTRACT

Catalytic membrane reactors have the advantages of allowing the selective removal of products, avoiding the separation procedure of powder catalysts from the reaction mixture, intensifying the diffusion of reactants in the catalytic region, and integrating different reactions in one unit. Catalytic membrane reactors have been widely applied in the fields related to carbon peaking and carbon neutrality, including the capture and utilization of carbon dioxide, hydrogen production, and hydrogenation reaction. This review summarizes the design and fabrication of catalytic membrane reactors, with the focus on the capture and efficient utilization of carbon dioxide, hydrogen production and efficient liquid-phase hydrogenation. The design of membrane materials, catalyst materials and catalytic membranes, and the operation of catalytic membrane reactors are discussed respectively. Finally, the perspectives and future challenges of catalytic membrane reactors for carbon peaking and carbon neutrality are forecasted.

1. Introduction

Reaction and separation processes are fundamental elements of the chemical industry [1–5]. Their efficiency significantly impacts energy consumption, material utilization, and ecological environment of manufacturing chemical products [5]. In general, the two processes operate independently, resulting in a long process, high energy consumption, and low production efficiency. Therefore, integratng reaction and separation processes in one unit has emerged as an important development direction in the chemical industry, which can potentially improve quality of products, enhance production efficiency, and minimize environmental pollution.

Catalytic membrane reactors (CMRs) couple the reaction and separation processes within a single unit (Fig. 1), which have the following advantages [1,2,6,7]: (1) Allowing selective removal of products. Through selective removal of some reaction products from reaction system, the limitation of thermodynamic equilibrium will be overcome, which is conducive to drive chemical balance to the direction of product formation, greatly improving the conversion and product selectivity of reaction; (2) Avoiding separation procedure of powder catalysts from

* Corresponding author.
** Corresponding author. State Key Laboratory of Catalysis, Dalian Institute of Chemical Physics, Chinese Academy of Sciences, 457 Zhongshan Road, Dalian, 116023, China.
*** Corresponding author.
**** Corresponding author.
E-mail addresses: zhuxf@dicp.ac.cn (X. Zhu), huangash@chem.ecnu.edu.cn (A. Huang), jianghq@qibebt.ac.cn (H. Jiang), rizhichen@njtech.edu.cn (R. Chen).
[1] These authors equally contribute to this work.

https://doi.org/10.1016/j.advmem.2023.100070
Received 28 July 2023; Received in revised form 21 September 2023; Accepted 21 September 2023
Available online 21 October 2023
2772-8234/© 2023 The Authors. Publishing services by Elsevier B.V. on behalf of KeAi Communications Co. Ltd. This is an open access article under the CC BY-NC-ND license (http://creativecommons.org/licenses/by-nc-nd/4.0/).

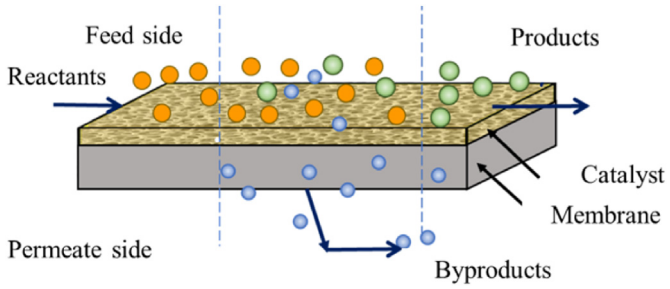

Fig. 1. Schematic illustration of the catalytic membrane reactor.

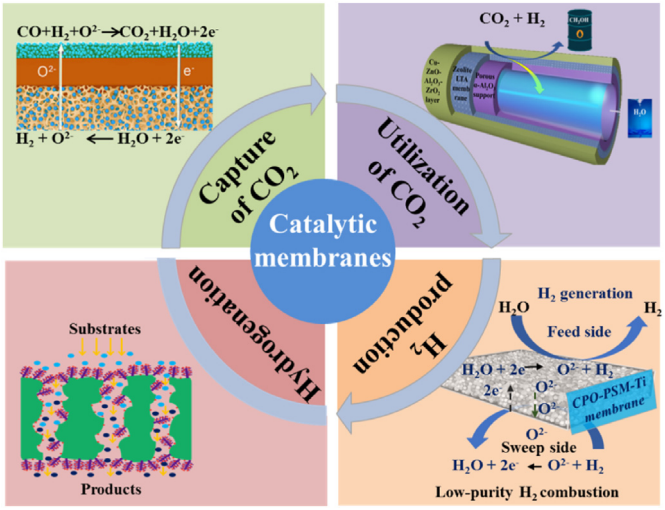

Fig. 2. Schematic illustration of the CMRs applied in carbon peaking and carbon neutrality.

reaction mixture; (3) Intensifying the diffusion of reactants in the catalytic region, and then the reaction rate is accelerated; (4) Coupling different reactions in one unit, which improves the reaction efficiency.

Gryaznov [8] was the first to propose the concept of CMRs in 1963 based on the dense membranes, attracting a wide interest. Hsieh et al. [9] developed the porous catalytic membrane in the 1980s, in which the catalyst was placed exclusively as a thin surface layer on the membrane. In the CMR based on the developed porous catalytic membrane, the gas was fed from the catalyst side and the liquid was supplied at the same pressure from the support side so as to improve the catalytic performance. However, the CMRs were still regarded as a concept with less investigation in the early 1990s [10]. Over the last two decades, significant advancements have been made in the field of CMRs, primarily due to the development of advanced membrane materials, such as zeolite membranes, mixed ionic-electronic conducting membranes, and metal membranes. The remarkable development of membrane materials has enabled the CMRs to achieve a massive range of applications including the capture and utilization of carbon dioxide, hydrogen production, and hydrogenation (Fig. 2) [1,2,6,7,11–13].

Although the CMRs have been widely applied in the fields related to carbon peaking and carbon neutrality [14–18], there is almost no review that comprehensively describes the progresses. Herein, the recent progresses in the CMRs applied in carbon peaking and carbon neutrality (Fig. 2) are reviewed, including the design and preparation of membrane materials, catalyst materials and catalytic membranes, and the fabrication and operation of CMRs. And, the perspectives and future challenges of CMRs for carbon peaking and carbon neutrality are proposed.

2. CMRs for CO_2 capture

Coal-fired power plants account for about 30% of the world's total CO_2 emissions [19,20]. Therefore, CO_2 capture is particularly important in the power plants. The integrated gasification combined cycle (IGCC) is a clean coal-based power generation technology as well as a promising pre-combustion CO_2 capture technology when coupled with carbon capture. The IGCC system with CO_2 capture contains several main units. The gasification unit involves converting the fuel into raw syngas at elevated temperatures (950–2000 °C) and pressures (10–80 bar) in the presence of steam and oxygen [21]. The produced mixtures are quenched/scrubbed to remove pollutants and impurities, and then the cleaned syngas is converted into CO_2 through the water gas shifting reaction (WGS). Next, CO_2 and H_2 are separated. The last parts are the CO_2 capture unit and power generation unit consisting of a gas turbine combustor and a steam turbine combustor.

The net efficiency of the IGCC system decreases approximately 7–12% due to the CO_2 capture process [22–26]. Many efforts have been made to lower the energy penalty related to CO_2 capture. For example, coupling membrane reactors (MRs) to the IGCC process are proposed, because MRs fulfill process intensification and result in higher efficiencies and lower costs by combining separation and reaction in one unit. The high purity oxygen used in the gasification unit is usually obtained through oxygen transport membranes (OTMs) in the air separation

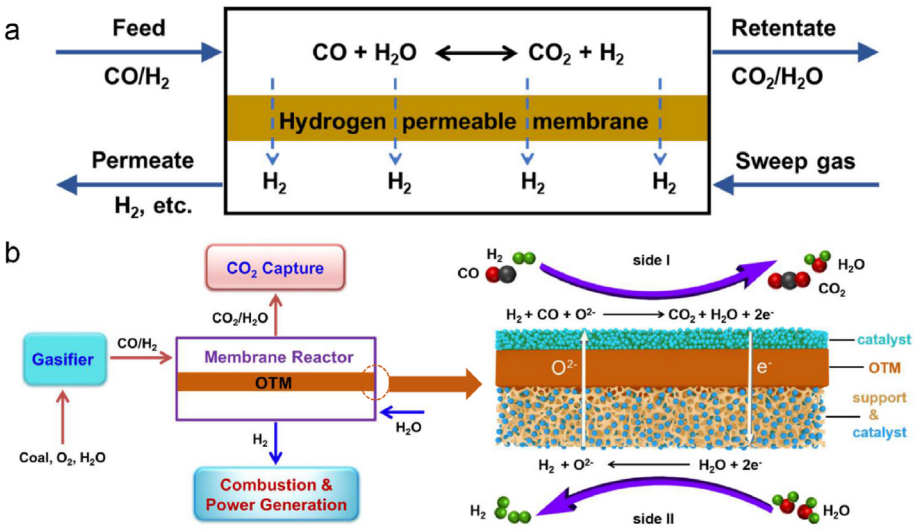

Fig. 3. Working principle of membrane reactors for CO_2 capture. (a) Hydrogen permeable membrane, (b) OTM. Reprint from Ref. [17].

Table 1
The hydrogen production performance of some representative OTMs.

Membrane material	Thickness (mm)	T (°C)	Condition at both sides	Catalyst at water side	Hydrogen production rate (mL cm^{-2} min^{-1})	Ref.
$La_{0.3}Sr_{0.7}FeO_{3-\delta}$ (LSF)	3.00	860	17% H_2O; CO		0.015	[39]
$La_{0.7}Sr_{0.3}Cu_{0.2}Fe_{0.8}O_{3-\delta}$ (LSCF)	0.02	900	49%H_2O; 99.5%CO	–	~4.7	[40]
$BaFe_{0.9}Zr_{0.1}O_{3-\delta}$ (BFZ)	1.56	900	49%H_2O; 99.5%CO	–	3.2	[41]
$Ba_{0.98}Ce_{0.05}Fe_{0.95}O_{3-\delta}$ (BCF)	0.50	900	90%H_2O; 50% CO and 50% H_2	Ru/SDC	6.7	[42]
$Ce_{0.85}Sm_{0.15}O_{1.925}$– $Sm_{0.6}Sr_{0.4}Al_{0.3}Fe_{0.7}O_{3-\delta}$ (SDC-SSAF)	0.04	900	90%H_2O; 80% H_2	Ru/SDC	15.5	[43]
$Ce_{0.85}Sm_{0.15}O_{1.925}$– $Sr_2Fe_{1.5}Mo_{0.5}O_{6-\delta}$ (SDC-SFM)	0.50	900	90%H_2O; 80% H_2	Ni/SDC	6.3	[45]
$Ce_{0.85}Sm_{0.15}O_{1.925}$– $Sm_{0.6}Sr_{0.4}Cr_{0.3}Fe_{0.7}O_{3-\delta}$ (SDC-SSCF)	0.04	900	90% H_2O; 50% CO and 50% H_2	Ni/SDC	14.2	[17]
SDC-SSCF	0.04	940	90% H_2O; 50% CO and 50% H_2	Ni/SDC	17.7	[17]
$La_{0.9}Ca_{0.1}FeO_{3-\delta}$ (LCF-91)	0.90	990	50%H_2O; 5%CH_4	–	0.5	[47]
$Ce_{0.9}Pr_{0.1}O_{2-\delta}$– $Pr_{0.1}Sr_{0.9}Mg_{0.1}Ti_{0.9}O_{3-\delta}$ (CPO-PSMTi)	0.70	900	88%H_2O; 40%H_2	–	3.4	[48]
$BaZr_xCo_yFe_zO_{3-\delta}$ (BZCF)	0.17[a]	900	75%H_2O(g); 4%CH_4	–	2.2	[15]
$Gd_{0.2}Ce_{0.8}O_{1.9-\delta}$– $Gd_{0.08}Sr_{0.88}Ti_{0.95}Al_{0.05}O_{3\pm\delta}$ (GDC-GSTA)	1.1	900	25%H_2O(g); 50%H_2	–	2.0	[52]

[a] The thickness here refers to the wall thickness of the hollow-fiber membrane.

process. Process simulation indicates the power generation efficiency is improved by only 1% point [27,28]. Membrane reactors were proposed for CO_2 capture in the IGCC process. Several membranes such as MOF, polymeric and supported molten-salt membranes exhibit high CO_2 selectivity. However, MOF and polymeric membranes are mainly limited to low temperature applications, due to their poor thermal stability. The supported molten-salt membranes, where the molten carbonate was supported by a porous solid phase scaffold, can be operated at high temperatures of up to 1000 °C. The porous solid phase consists of ionic and/or electronic conductors. Some work including materials selection and properties, fundamental mechanisms, materials advancements, performance limiting factors, and novel membrane reactor designs have been reviewed before [29,30]. These results will not be repeated in this review. The application of hydrogen and oxygen permeable membranes in the IGCC process will be discussed in detail, and are illustrated in Fig. 3. Polymer membranes, dense proton conducting membranes and Pd-based composite membranes were proposed to separate H_2 from the products of WGS reaction in the IGCC process (IGCC-WGS, Fig. 3a) [21, 31–35]. After complete separation of H_2 in the membrane reactors, the retentate mainly consisting of CO_2 and H_2O is condensed. Finally, high concentration and purity CO_2 is ready for compression and capture.

In the case of polymer membranes, process simulation indicates CO_2/H_2 separation degrees above 85% and CO_2 purities above 95% must be reached to achieve an efficiency loss of less than 10% [21]. However, the current selectivity and permeability of polymeric membranes for H_2/CO_2 separation still need to be improved to reach the goals. Pd-based composite membranes are 100% selective to hydrogen and have high hydrogen permeability, but they are relatively expensive and sensitive to H_2S contained in the syngas [6,36]. In order to stably operate Pd membranes, the processes of removing H_2S and quenching the gasifier product to 400 to 500 °C are needed. Process simulation shows the corresponding energy penalty is approximately 8% [37].

Recently, a novel IGCC-OTM concept (Fig. 3b) was proposed to fulfill precombustion CO_2 capture with improved carbon capture efficiency [17,38]. In the IGCC-OTM system, syngas produced from the gasifier and steam are fed separately to both sides of OTM. On one side, the steam dissociates to H_2 and oxygen at elevated temperature. OTM only permits the oxygen ions to permeate through the membrane to the other side and interact with the syngas. Therefore, the hydrogen selectivity in theory is deemed to be 100%. The syngas is oxidized to CO_2 and water. After condensation, CO_2 with high concentration and purity is collected and captured. Finally, the hydrogen produced through steam dissociation, along with any remaining unconverted steam, are introduced into both the gas turbine and steam turbine to generate electricity. The overall process happened in the OTM reactor comprises both WGS reaction and H_2/CO_2 separation. Process simulation results show that the novel IGCC-OTM system simplifies the whole process, improves the heat integration and increases the power generation efficiency by 3–4% points [38].

At present, most of the researches on IGCC system combined with CO_2 capture are limited to process simulation. In order to realize industrial applications, efforts should be focused on the design of MRs, which include membrane materials, catalysts, and the coupling interaction principle between reactions and separation. In the water dissociation process, in order to promote hydrogen production, it is crucial to quickly remove the generated oxygen and shift the equilibrium. Thus, membrane materials must exhibit exceptional oxygen permeability, and the water dissociation and syngas (H_2 and CO) oxidation reactions should be accelerated. There are many researches on the OTM reactors suitable for the IGCC-OTM process. Therefore, recent progresses on the development of OTM materials and catalysts, and the design of OTM reactors for CO_2 capture are outlined.

2.1. *Preparation of membrane materials for CO_2 capture*

The membrane reactors in IGCC-OTM fulfills H_2 production and syngas oxidation in one unit. Water dissociation reaction rate, oxygen permeability of OTMs and syngas oxidation reaction rate are all the potential limiting steps for the MRs. The H_2 production rate equals to water dissociation rate and is 2 equiv to the oxygen permeation flux of OTMs. Therefore, hydrogen production rate is a paramount index to assess the performance of MRs. The oxygen permeability, chemical stability, mechanical strength, thermal expansion, and material cost of membrane all affect their applications in a practical system. Since the membrane is exposed to harsh atmospheres, the stability of OTMs for CO_2 capture plays a vital role in operation. Membrane materials should have enduring stability in a gas mixture that incorporate H_2S, H_2O(g), CO, CO_2, and H_2.

Single-phase membranes, mainly perovskite membranes exhibit relative high oxygen permeability, thus high hydrogen production rate. Some representative OTMs used for water splitting reaction are listed in Table 1. A 3.0-mm-thick $La_{0.3}Sr_{0.7}FeO_{3-\delta}$ (LSF) membrane showed about 0.015 mL cm^{-2} min^{-1} hydrogen production rate when 17% H_2O and pure CO were fed into two sides of the membrane at 860 °C, respectively [39]. The hydrogen production rate was three times that of He as the sweep gas. It directly proved that increasing oxygen partial pressure gradient benefited to the oxygen removal and thus increased the water decomposition rate. Park et al. fabricated $La_{0.7}Sr_{0.3}Cu_{0.2}Fe_{0.8}O_{3-\delta}$ (LSCF7328) [40] and $BaFe_{0.9}Zr_{0.1}O_{3-\delta}$ (BFZ) [41] membranes to produce

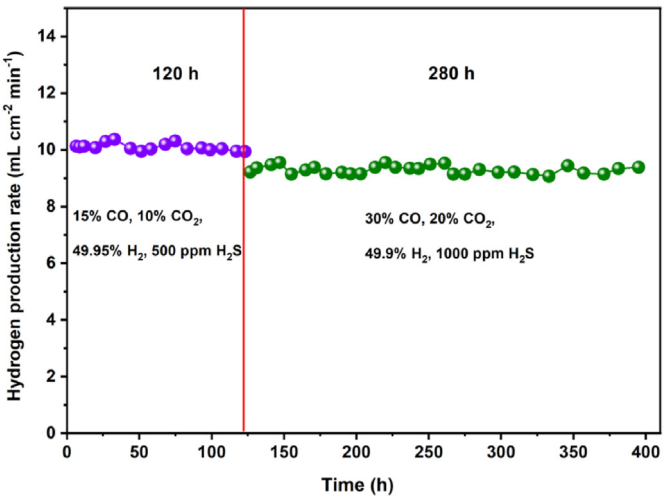

Fig. 4. Long-term operation of SDC-SSCF membrane under various atmospheres at 900 °C. Reprint from Ref. [17].

hydrogen via coal-gas-assisted water splitting. With 49% H_2O and 99.5% CO flowing on two sides of the 0.02-mm-thick LSCF and 1.56-mm-thick BFZ membranes, the production rates of hydrogen reached 4.7 and 3.2 mL cm^{-2} min^{-1} at 900 °C, respectively. The rates of hydrogen production exhibited a decrease as the concentration of CO_2/CO was raised, partly due to the increase of oxygen partial pressure. LSF, LSCF and BFZ are cobalt-free materials, while their long-term stabilities were not reported in literature. The hydrogen production rate of 0.5-mm-thick $Ba_{0.98}Ce_{0.05}Fe_{0.95}O_{3-\delta}$ (BCF) membrane reached ~6.7 mL cm^{-2} min^{-1} with 13.5% CO conversion at 900 °C when 200 mL cm^{-2} min^{-1} dilute steam ($H_2O/N_2 = 9/1$) and 50 mL cm^{-2} min^{-1} syngas ($CO_2/H_2 = 1/1$) were fed into two sides of the membrane, respectively [42]. However, the hydrogen production rate decreased by about 10% after operation for about 100 h due to the instability of BCF membrane. CO, CO_2 and H_2S are highly toxic to many membranes. Therefore, membranes with good stability in atmospheres containing H_2S, H_2O(g), CO, CO_2 and H_2 need to be developed.

Dual-phase membranes facilitate the transportation of oxygen ions and electrons in separate phases, usually have relative high stability. Li et al. reported a $Ce_{0.85}Sm_{0.15}O_{1.925}$–$Sm_{0.6}Sr_{0.4}Al_{0.3}Fe_{0.7}O_{3-\delta}$ (SDC-SSAF) membrane exhibiting stable hydrogen production rate in the H_2, H_2O(g) and H_2S (100 ppm) conditions for about 200 h [43]. It also has good stability in the MRs for partial oxidation of methane (POM), in which air and methane were supplied into two sides of the OTM, respectively [44]. The stability in CO_2-containing atmospheres was not reported in this study. Later, Cai et al. developed CO_2- and H_2S-tolerance membranes, $Ce_{0.85}Sm_{0.15}O_{1.925}$–$Sr_2Fe_{1.5}Mo_{0.5}O_{6-\delta}$ (SDC-SFM) [45] and $Ce_{0.85}Sm_{0.15}O_{1.925}$–$Sm_{0.6}Sr_{0.4}Cr_{0.3}Fe_{0.7}O_{3-\delta}$ (SDC-SSCF) [17]. The rate of hydrogen production in the 0.5-mm-thick SDC-SFM membrane reached 5.3 mL cm^{-2} min^{-1} at 900 °C. When CO_2 was added to the sweep side, it adsorbed on the membrane surface and reduced the rate of hydrogen production. But the rate of hydrogen production maintained at a fixed value for long time and fully recovered when CO_2 was removed. It demonstrated the CO_2 adsorption was weak and reversible. The performance was almost unaffected by H_2S. Meanwhile, there was no synergistic side effect between CO_2 and H_2S on the SDC-SFM MR [45]. Similar results were obtained on SDC-SSCF membranes. Meanwhile, the SDC-SSCF membrane showed good POM performance and stability [46]. In order to better adapt to the operating conditions in the IGCC-OTM process, Cai et al. verified the feasibility of SDC-SSCF membrane under harsh conditions of a gas mixture that simulated coal gasification products with 30% CO, 20% CO_2, 49.9% H_2 and 1000 ppm H_2S [17]. As shown in Fig. 4, the SDC–SSCF membrane exhibited unprecedented stability for 400 h on-stream. Besides, the hydrogen production rate of the 38 μm-thick asymmetric SDC–SSCF membrane with dense layer and Ni/SDC catalyst reached 17.7 mL cm^{-2} min^{-1} at 940 °C when 90% water and syngas ($H_2/CO = 1$) were supplied into the two sides of membrane, separately. This is the first OTM shows great potential in IGCC-OTM process for CO_2 capture.

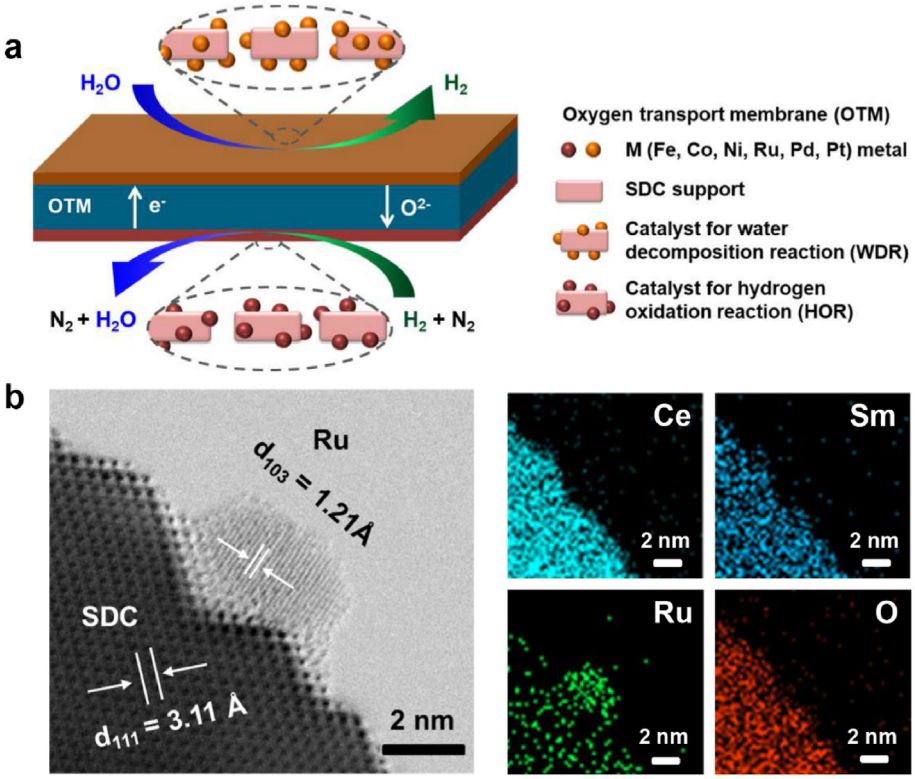

Fig. 5. Catalysts in the OTM reactor. (a) Schematic, (b) reduced fresh Ru/SDC catalyst. Reprint from Refs. [53,54].

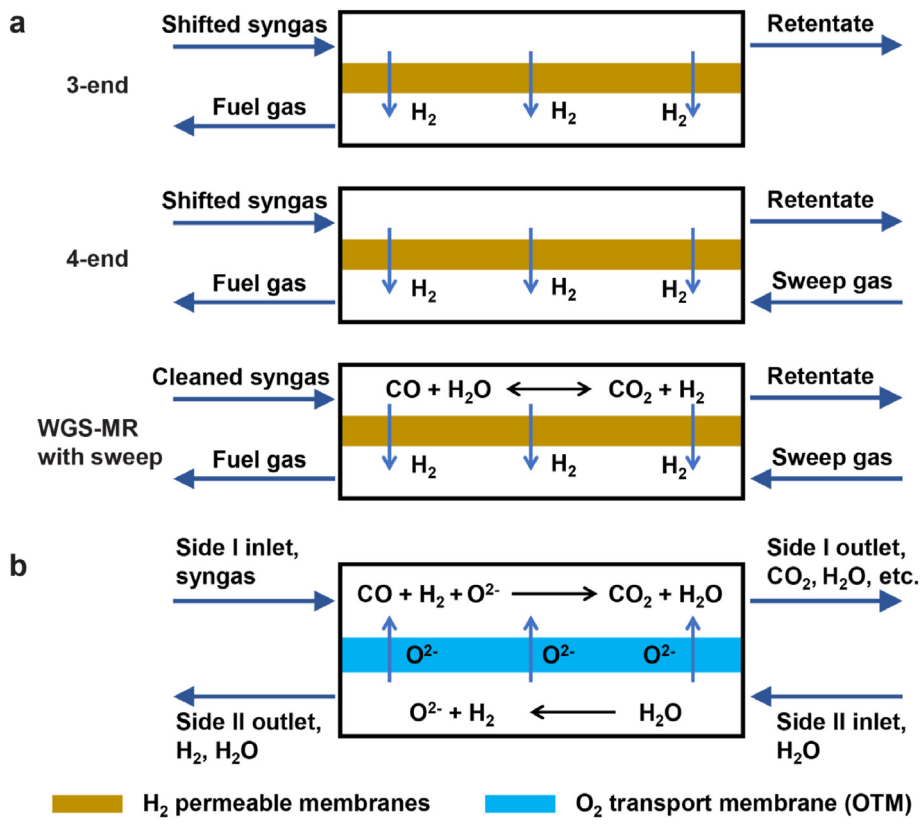

Fig. 6. Schematic graphs of different membrane integration modes. (a) Hydrogen permeable membrane, (b) oxygen transport membrane.

Other studies on OTM reactors were usually related to water dissociation coupled with POM or hydrogen oxidation reactions, which have been reviewed in other papers and are not described in detail here. Some of them exhibited relative low hydrogen production rates, such as $La_{0.9}Ca_{0.1}FeO_{3-\delta}$ [47]. $Ce_{0.9}Pr_{0.1}O_{2-\delta}$–$Pr_{0.1}Sr_{0.9}Mg_{0.1}Ti_{0.9}O_{3-\delta}$ membrane exhibited high stability, but low hydrogen production rate of 0.52 mL cm^{-2} min^{-1} at 940 °C [48]. Thus, one of the key issues for the MR is to break the trade-off limitation between permeability and stability of membrane materials. Besides developing new membrane materials, decreasing membrane thickness or optimizing membrane structures can also improve hydrogen production rates. It is common to prepare asymmetric membranes or hollow-fiber membranes to reduce the bulk diffusion resistances, thus improving the permeability. Li and Cai et al. studied the influences of the bulk diffusion resistance and surface reaction resistance by different structural types in SDC-SSAF [49] and SDC-SSCF [50] membrane reactors. For most cases, the surface reaction resistance and bulk diffusion resistance jointly control the overall performance. The concentration polarization resistance in porous support layer of the asymmetric membrane cannot be ignored due to the high reaction and permeation rates. Experiments demonstrated grooving in the porous layer was a favorable approach towards lowering the polarization concentration and upgrading the hydrogen production efficiency [51]. Further works on upscaling OTMs and membrane modules are needed for industrial applications.

2.2. *Preparation of catalysts for CO_2 capture*

Water dissociation and syngas oxidation reactions happen at two sides of OTMs. The reaction kinetics of these two reactions can be promoted by applying active catalysts on the membrane surface. Most studies focused on developing new membrane materials and changing membrane structures. Only few papers expressed growing concern over the development of catalysts suitable for hydrogen oxidation reaction and water dissociation reaction.

In early studies, there were no catalysts in LSCF [40], BZCF [15], and $Gd_{0.2}Ce_{0.8}O_{1.9-\delta}$ – $Gd_{0.08}Sr_{0.88}Ti_{0.95}Al_{0.05}O_{3\pm\delta}$ [52] membrane reactors. Hence, the corresponding hydrogen production performance was low, shown in Table 1. Cai et al. developed M/SDC (M = Fe, Co, Ni, Ru, Pt, Pd) catalysts [50,53,54] for SDC-SSCF MRs to promote the hydrogen oxidation reaction and water dissociation reaction illustrated in Fig. 5. Ni/SDC catalyst had the highest performance among the non-noble metal catalysts [50]. Under harsh conditions containing CO, CO_2, H_2 and H_2S with high concentrations, Ni/SDC catalyst showed good stability in the long-term test [17]. To construct strong interactions between metals and supports, in-situ exsolved Ru/SDC nano-catalyst was developed (Fig. 5b). When Ru catalyst was coated on both sides of asymmetric SDC-SSCF membrane, a maximum hydrogen production rate of 21.6 mL cm^{-2} min^{-1} at 900 °C was obtained, which was twofold compared with that of with Ni-based catalysts and comparable to the permeation flux of Pd-based membranes [53]. Experiment results demonstrated Ru, Pt, Pd/SDC catalysts had different catalytic activities toward the hydrogen oxidation reaction and water dissociation reaction. After testing for tens of hours, Ru NPs with a size range of 3–5 nm ultimately grew to a diameter of less than 20 nm, but a degradation of MR performance was not observed [54]. At present, the research about catalysts in MR for CO_2 capture is still in the initial stage. Future work is needed to design catalysts with higher activity for the water decomposition reaction and syngas oxidation reaction, respectively. The composition and cost of catalysts need to be optimized for the applications on CO_2 capture in the MRs.

In general, there are few researches that specifically addresses the advancement of catalysts for OTM reactors. In order to accelerate the hydrogen production process, it requires more efforts to design catalysts on combining theoretical calculations and advanced characterization

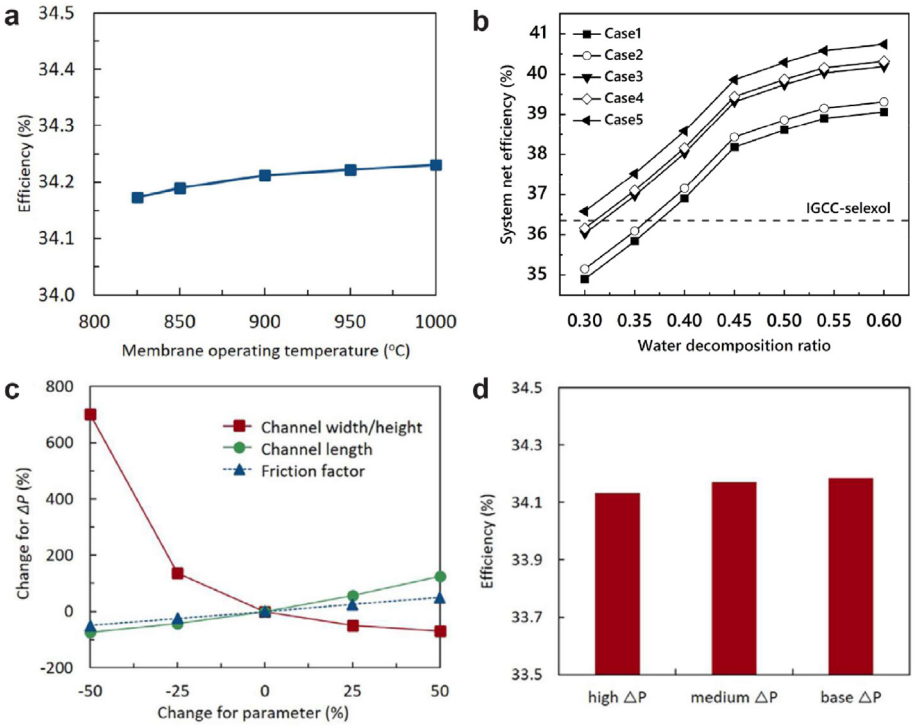

Fig. 7. Simulation results. (a) The dependence of system efficiency on the operating temperature of the membrane reactor [38], (b) influence of water decomposition ratio [57], (c) sensitivity of the pressure drop to the channel width/height, channel length, and friction factor [38], (d) the system efficiency decreased with increasing pressure drop (high ΔP = 1 bar and medium ΔP = 0.5 bar for both feed and sweep sides) [38]. Reprint from Refs. [38,57].

methods. Following rules should be considered when designing new catalysts. Catalysts have the potential to undergo reactions with the membrane materials at high temperature during the long-term operation, destroying the stability of MRs. Supported catalysts that transfer both electrons and oxygen ions are more suitable in the MRs, which benefit the oxygen supply or removal. More strategies need to be proposed to inhibit the growth and sintering of nanoscale active centers.

2.3. Design of CMRs for CO_2 capture

Besides membrane materials and catalysts, the performance of MRs is also affected by the membrane configuration, packing structure of catalysts, module design and operation mode [55,56]. Membrane configuration includes planar, tubular, and hollow fiber types. In planar MRs, the contact time between the reactants and membranes is short and the membrane area is limited. The water conversion ratio and hydrogen production rate are not very high. Better performance can be obtained by using tubular MRs under higher operating pressures. The tube diameter, thickness and porosity of support and thickness of dense layer should be optimized according to the operation conditions such as pressure, concentration and flow rates of steam and syngas.

The morphology and loading mode of catalysts also affect the performance of MRs. Catalysts can be loaded in MRs in several ways. The common way is coating the catalyst slurry onto the membrane surface. The thickness and porosity of the catalyst layer may affect the performance of MRs. In order to increase the contact time between reactants and catalysts, additional pelletizing catalysts are sometimes needed to be packed into MRs. For asymmetric membranes with porous supports, catalysts can be loaded into the porous supports by impregnation method or directly mixed with the porous supports when preparing membranes. The performance of SDC-SSCF membrane with Ni precursor added in the tape-casting slurry of porous support was lower than that of membrane with Ni catalyst loaded by impregnation method [17]. It may be ascribed to the growth of NiO particles to large sizes during the high temperature calcination step of the membrane preparation. The membrane with more catalysts loaded by impregnation method showed lower performance, which indicated the concentration polarization resistance caused by different porosity influenced the performance. In the published studies, different membrane materials with different membrane configurations have been prepared, respectively. However, the influence of MR type on the hydrogen production has not been directly investigated, and the interaction between the membranes and catalysts are still not well illustrated.

Schiebahn et al. compared the advantages and disadvantages of IGCC-WGS as a three- or four-end module (Fig. 6a) [35]. High CO conversion is demanded in the three-end module, since unconverted CO is not separated, resulting in a loss of heating value for the gas turbine. In the four-end module, sweep gas is utilized in the hydrogen permeation side, which reduces the partial pressure of H_2 and is feasible in the IGCC process since the sweep gas will act as a diluent in the gas turbine combustor unit with low NO_x emissions. It has also been pointed out that countercurrent design in the four-end module of IGCC-OTM reactor (Fig. 6b) can sustain the gradients on both ends and obtain high conversion [17,38].

2.4. Coupling interaction and energy evaluation of CMRs for CO_2 capture

Temperature and operation conditions affect the performance and energy efficiency of MRs for CO_2 capture. The key substeps that determine the performance of MRs, including water dissociation, syngas oxidation, and ambipolar transport of electrons and oxygen ions, are activated by thermal energy. Usually, the performance is better at higher temperatures. The production rate of hydrogen, conversion ratios of water, CO and H_2 all increased from 750 to 940 °C at the same operating conditions [17]. The hydrogen production rate and water conversion ratio increase with the increase of flow rate of syngas, while CO and H_2 conversion ratios decrease. Just as mentioned above, the conversion rate of CO cannot achieve a high level due to the scarce contact time of the reactant gases in the MRs. Nevertheless, the conversion ratios of CO and H_2 at 900 °C reached 41% and 54%, respectively [17]. By implementing

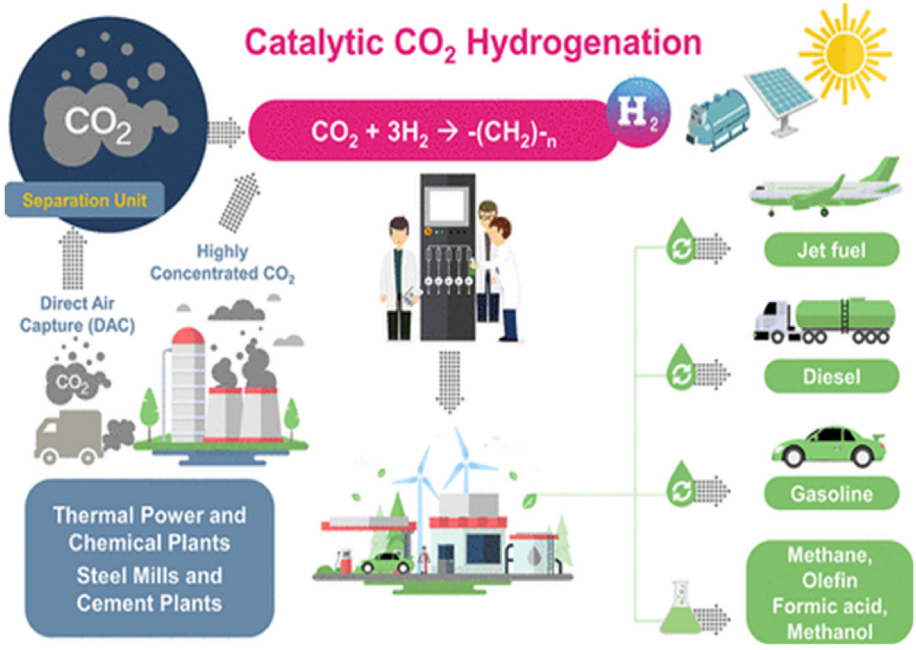

Fig. 8. Scheme of catalytic CO_2 hydrogenation to high-value fuels and chemicals. Reprint from Ref. [63].

an optimized operational model, it is possible for syngas to be converted entirely into water and CO_2.

The energy penalty of the IGCC-OTM process for CO_2 capture was analyzed by simulations. Wu et al. constructed three models of different IGCC processes, i.e., IGCC-REF (without CO_2 capture), IGCC-WGS and IGCC-OTM [38]. Simulation results showed that the overall efficiency of IGCC-OTM system was 34.2%, lower than that of the same IGCC system without CO_2 capture (37.4%), and better than the IGCC-WGS system (30.6%). Meanwhile, the specific primary energy consumption for CO_2 avoided (SPECCA) of IGCC-OTM was only 1.08 MJ $kgCO_2^{-1}$, showcasing a 59.4% reduction compared to the IGCC-WGS system [38]. As shown in Fig. 7a, the system efficiency of the IGCC-OTM process was reduced slightly when the operational temperature decreased from 1000 to 825 °C. Chi et al. constructed five cases of different IGCC-OTM processes at different WGS MR operation temperatures and inlet temperatures [57]. The system achieved a net efficiency of 38.9% with a 100% CO_2 capture ratio, which is approximately 2.6% points higher than the IGCC-Selexol system with a 90% CO_2 capture ratio, when the operation temperature of WGS MR was 900 °C and the water decomposition ratio was 0.5. High water conversion ratio is beneficial to the net efficiency of the system. The net efficiency of the system increased by about 4.1% points when the water conversion ratio increased from 30% to 60% based on the process simulation results (Fig. 7b). In order to guarantee the net efficiency higher than that of IGCC with the Selexol process, the water conversion ratio should be above 38% at 900 °C [57].

Simulation results also showed that the pressure drop exhibits a substantial dependence on reactor design factors, including channel length and size [38]. As shown in Fig. 7c, the channel width/height of a simplified square-shape monolith MR had the largest influence on the drop of pressure. The higher the pressure drop in the OTM reactor, the lower the efficiency of the IGCC-OTM system for CO_2 capture. When the pressure drop in the MR was 1 bar, the difference is −0.05% compared to the base of negligible pressure (Fig. 7d).

All the simulation results show that the IGCC-OTM process has great potential for precombustion of CO_2 capture. Further works on experimental and simulation results will both lay a foundation for the practical applications of the system.

3. CMRs for efficient utilization of CO_2

The exploitation and use of fossil fuels such as natural gas, oil and coal have brought unprecedented opportunities for human development. However, the massive use of fossil fuels has also contribute to a sharp increase of the concentration of greenhouse gases such as CO_2 in the atmosphere. In 2018, the global CO_2 emissions reached 330 billion tons, and the atmospheric concentration of CO_2 has increased from 280 ppm pre-industrial revolution to 410 ppm. As a major greenhouse gas, the increase of CO_2 concentration causes a severe greenhouse effect, leading to global warming, sea level rise, ocean acidification and other environment and climate problems, and has become a huge challenge for human survival and sustainable development in the future. The reduction of CO_2 emission has become a global concern [58]. Therefore, it is of great significance to explore efficient, green and economical CO_2 capture, recovery, conversion and utilization technologies to reduce CO_2 emissions. Compared with CO_2 capture and storage technologies, CO_2 catalytic hydrogenation to high-value and sustainable chemicals (such as methanol, dimethyl ether, ethanol, dimethyl carbonate, etc.) through chemical reaction is the most promising method for efficient conversion and utilization of CO_2 (Fig. 8) [59–64]. Among these high-value chemicals, methanol is not only a sustainable liquid fuel with excellent combustion performances, but also an important raw material for the preparation of aromatics, gasoline, olefins and other high-value chemicals (such as dimethyl, acetic acid and formaldehyde ether). Therefore, catalytic conversion of CO_2 into methanol ($CO_2 + 3H_2 \leftrightarrows CH_3OH + H_2O$) is considered to be the most attractive way in CO_2 utilization, which not only helps to reduce CO_2 emissions, but also realize carbon cycle. Therefore, the studies on CO_2 catalytic conversion to methanol have sparked extensive attention in recent twenty years [65–73].

3.1. *Catalysts for efficient utilization of CO_2*

CO_2 can be converted to other useful chemicals and fuels through mineralization, biochemical, photocatalytic, electrocatalytic and thermocatalytic reactions. Among these pathways, CO_2 electrocatalytic reduction has drawn great attention due to its friendly reaction conditions, minimized chemical consumption, and easy-to-scale-up applications, which offers a sustainable and promising way to reduce CO_2

emissions [74–78]. Recently, a great number of electrocatalysts have been proposed for the CO_2 reduction, such as noble metals, transition metals, metal oxides, metal alloys, and carbon-based materials. However, electrocatalytic CO_2 reduction is a rather complex process involving multiproton-coupled electron transfer, leading to the difficulty to control the reduction products. Further, it is still difficult to develop a selective, scalable, and stable electrocatalyst for the CO_2 reduction because of the insufficient understanding of the mechanistic reduction process, thus inhibiting its industrial applications.

Besides the CO_2 electrochemical reduction, CO_2 conversion is widely carried out by thermocatalytic reduction, including direct CO_2 catalytic hydrogenation and CO_2 conversion to CO ($CO_2 + H_2 \leftrightarrows CO + H_2O$) by reverse water-gas shift (RWGS), followed by Fischer Tropsch (F-T) synthesis. The RWGS is an endothermic reaction with a standard formation enthalpy of 42.1 kJ/mol at 25 °C. Thus it requires a high temperature to drive the equilibrium conversion to CO. While the direct CO_2 catalytic hydrogenation to methanol is an exdothermic reaction with a standard formation enthalpy of −49.3 kJ/mol at 25 °C. Therefore, this CO_2 conversion process can be usually realized at moderate pressure (5–10 MPa) and temperature (200–300 °C). The development of highly active, selective and stable catalysts for CO_2 hydrogenation to methanol is still challenging.

In the past 20 years, considerable endeavors have been undertaken to investigate catalysts with high activity for the conversion of CO_2 to methanol through hydrogenation. The catalysts used for CO_2 catalytic conversion to methanol mainly include noble metal catalysts, copper-based catalysts, metal oxide catalysts and metal alloy catalysts [65–73]. Although noble metal catalysts have high catalytic activity and selectivity, they cannot be widely used because of their high cost. Similar to syngas to methanol ($CO + 2H_2 \leftrightarrows CH_3OH$), copper-based catalysts are widely used for CO_2 catalytic hydrogenation to methanol on account of their relatively high catalytic activity and low preparation cost. Especially, Cu/ZnO catalysts play an important role in methanol synthesis. However, due to the competitive reverse water-gas shift reaction ($CO_2 + H_2 \leftrightarrows CO + H_2O$) and catalyst deactivation caused by by-product water during CO_2 catalytic hydrogenation to methanol, the catalytic performance of catalysts is still unsatisfactory for industrial applications. Therefore, the development of highly active, selective, water tolerant and stable Cu/ZnO based catalysts is highly desired for the conversion of CO_2 to methanol. In order to overcome these defects of the Cu/ZnO catalysts, metal oxides such as aluminum, zirconia, indium oxide, gallium oxide, cerium oxide, magnesium oxide, lanthanum oxide, or noble metals are often doped with the Cu/ZnO catalysts to enhances the Cu dispersion and stability, while the acid-base and redox properties can be modified through a variety of techniques, leading to improved activity and stability of Cu/ZnO catalysts [70,79–82].

ZrO_2 is a widely studied dopant of the Cu/ZnO catalysts for conversion of CO_2 to methanol. Normally, ZnO is helpful to improve the dispersion of Cu nanopaticles, and both ZnO and ZrO_2 are helpful to increase the CO_2 adsorption capacity. Further, the interface between metal and oxide [79] and the collaboration between Cu sites and hydroxyl groups of ZnO as well as the basic Lewis sites of ZrO_2 [80] also play key roles in the enhancement of catalytic activity. Therefore, ZrO_2 incorporated Cu/ZnO catalysts display a higher catalytic performance in CO_2 conversion to methanol because of the outstanding high specific surface area, semiconductor properties as well as mechanical and thermal stability [81]. Wang et al. prepared a Cu/ZnO/ZrO_2 catalyst for CO_2 catalytic hydrogenation to methanol [70]. It was found that ternary Cu/ZnO/ZrO_2 catalyst showed higher CO_2 adsorption capacity and the ability to hydrogenate carbonate species into reaction intermediates (methoxy and formate) in comparison with binary Cu/ZnO or Cu/ZrO_2 catalysts. Therefore, the CO_2 conversion and methanol selectivity were greatly improved. At 220 °C and 3.0 MPa, the CO_2 conversion was 18.2% and the selectivity of methanol was 80.2%. Enhanced activity of the Cu/ZnO/ZrO_2 catalyst for CO_2 catalytic conversion to methanol was further improved with Y_2O_3 and Ga_2O_3 additives [82]. Attributing to a better dispersion of Cu and stronger synergistic interaction between metallic metal oxide and Cu, a high methanol yield could be obtained with Ga_2O_3 as additive. Ladera et al. demonstrated that $Ga_{0.3}$-doped Cu/ZnO/ZrO_2 catalysts were highly effective for the selective conversion of CO_2 to methanol with a methanol productivity of 512 g methanol $h^{-1}kgcat^{-1}$ at 523 K and 4 MPa [83]. Recently, CeO_2 has emerged as a new dopant with the Cu/ZnO catalysts for CO_2 adsorption and activation attributing to its specific structural properties derived from reversible valence changes ($Ce^{4+}$and Ce^{3+}) and oxygen vacancies [84]. Arena et al. reported that the doping of CeO_2 significantly improved the methanol yield and catalytic activity of the Cu/ZnO catalyst [85].

The Cu-based catalysts are usually prepared by the co-precipitation of nitrate salt precursors in a basic aqueous medium, followed by aging, collecting, washing, drying, calcination and reduction [81]. The differences in preparation methodologies and precursors have great effects on the surface and structural properties of the catalysts, which determine the efficiency, selectivity and stability of the catalysts. However, the preparation of Cu-based catalysts by co-precipitation easily leads to the aggregation of metal nanoparticles, thus reducing the activity of the catalysts. So far, several preparation techniques, such as reverse co-precipitation with ultrasound irradiation [86] and surfactant-assisted coprecipitation [87], have been proposed to enhance the activity of the catalysts. Qi et al. synthesized a Cu–ZnO–Al_2O_3 catalyst through bimetallic MOF template strategy [88]. Compared with the Cu–ZnO–Al_2O_3 catalyst prepared by traditional co-precipitation method, the Cu–ZnO–Al_2O_3 catalyst prepared by template method showed a higher CO_2 conversion and selectivity of methanol at 240 °C and 3.0 MPa.

Besides Cu-based catalysts, other catalysts like noble metal-based catalysts [89,90], metal alloy catalysts [91], oxides and hybrid oxide catalysts [69], have also been developed for conversion of CO_2 to methanol. Meng et al. developed a new and efficient $InNi_3C_{0.5}/Fe_3O_4$ catalyst for the conversion of CO_2 to methanol through the nano-loading of $InNi_3C_{0.5}$ intermetallic compound and the interaction of electronic metal carrier [73]. The single-pass conversion of CO_2 was up to 25%, and the selectivity of methanol was more than 90%. Recently, Liu et al. prepared Cu–$ZnFe_2O_4$ catalysts for CO_2 conversion to methanol [92]. The optimized 33Cu/ZnFe-0.5 catalyst obtained 9.4% CO_2 conversion and 71.6% selectivity of methanol at 300 °C and 4.5 MPa. Although significant progress has been made in improving the performance of catalysts for CO_2 hydrogenation to methanol, due to the high chemical inertness of CO_2 and the presence of many competitive reactions in CO_2 hydrogenation, the CO_2 conversion and methanol selectivity are still relatively low. In particular, the CO_2 hydrogenation to methanol reaction is reversible equilibrium, which is severely limited by the thermodynamic equilibrium. In the traditional fixed-bed reactor, the catalytic hydrogenation of CO_2 to methanol is greatly suppressed, resulting in the single-pass conversion of CO_2 is usually lower than 30%, and the methanol selectivity is lower than 70%. In addition, by-product water produced during CO_2 hydrogenation to methanol will accelerate the aggregation of catalyst nanoparticles, resulting in a significant reduction of the activity of the catalyst [93,94]. Thus, the demand for developing highly efficient, selective and stable catalyst for CO_2 hydrogenation to methanol remains high.

3.2. *Catalytic membranes for efficient utilization of CO_2*

Besides rational design of the highly efficient catalysts, the innovation in reactor design plays a significant role in view of the characteristics and challenges of the reaction of CO_2 hydrogenation to methanol. Membrane catalysis has the dual functions of catalytic reaction and product separation, thus it has many advantages that traditional catalytic reaction hardly matches [7]. However, it is challenging to design and build a catalytic membrane reactor with high catalytic activity and high thermal stability.

The by-product water is expected to selectively remove from the reaction system during CO_2 hydrogenation, therefore water selective

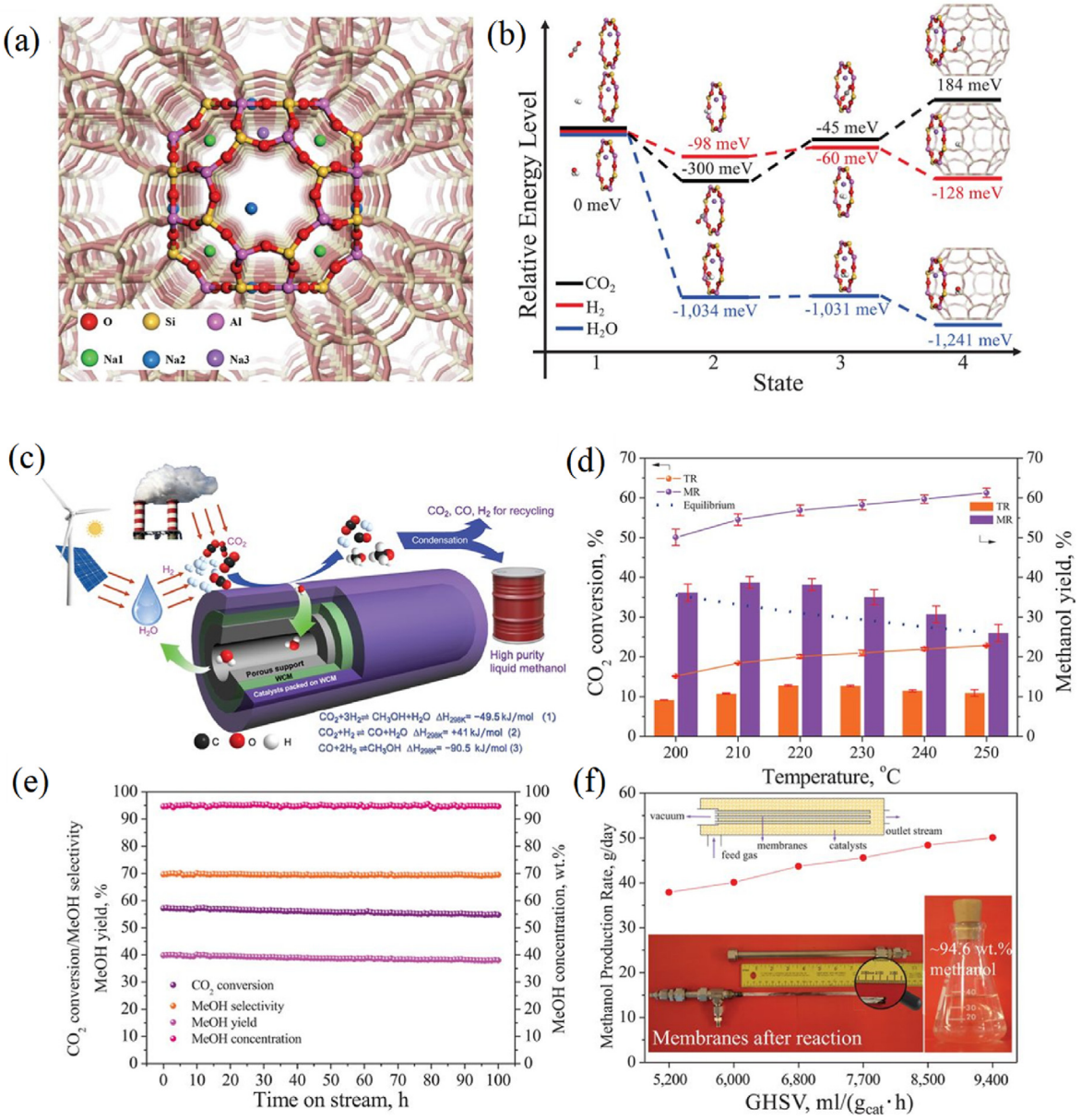

Fig. 9. DFT simulation (a, b) of the passage of molecules through NaA zeolitic channels. (a) Top view of the structural framework of NaA zeolite with three Na^+ sites in the dehydrated crystal structure. (b) The passage of molecules through the zeolitic channels of NaA. Schematics of the membrane reactor (MR) concept (c) and catalytic performance of the MR (d, e, f). Reprint from Ref. [3].

membranes are recommended to separate the by-product water. An evaluation was conducted on a commercially produced Nafion hollow fiber membrane for methanol synthesis by CO_2 hydrogenation for the first time at elevated pressures ($P < 30$ bar) and temperatures ($T =$ 160–200 °C) [95]. However, the stability of the polymeric membranes is unsatisfactory under a high reaction temperature and pressure, thus Nafion membranes are unfeasible for in-situ selective removal of by-product water in methanol produce from CO_2 hydrogenation. It is high desired to develop more stable membrane materials for the fabrication of CMRs. Zeolites are crystalline silicate or aluminosilicates microporous materials with three dimensional frameworks and uniform channels and periodic arrangements of cages. Since the pore size of zeolites is comparable to molecular dimensions (usually 3–10 Å), zeolites are able to exclude molecules larger than their pore aperture by molecular sieving. Due to their high thermal stability, uniform pore structure and strong acidity, zeolites are widely applied in separation and catalysis, thus opening a new road for the fabrication of CMRs. Firstly, zeolites have a single pore size and regular channel, thus the reactant or product molecules can be separated by molecular sieving or selective permeation. Secondly, zeolites have excellent acid catalytic activity. Finally, zeolites have high thermal stability to withstand hard catalytic reaction conditions such as high temperature and high pressure. Therefore, zeolite based CMRs have aroused great interest [3,16,96–104]. Most membrane catalysis applications are mainly concentrated on zeolite LTA, FAU and MFI membrane-based reactors, including the synthesis of methyl *tert*-butyl ether, esterification reaction, methane oxidation to syngas, ethylbenzene dehydrogenation, nitrobenzene dehydrogenation and CO_2 catalytic hydrogenation. In these reactions, the by-product water or hydrogen generated in the reaction is selectively separated through water or hydrogen selective zeolite membranes, thus breaking the thermodynamic balance and improving the reaction conversion.

Among these zeolite membranes, zeolite LTA membrane with Si/Al ratio of 1.0 has strong hydrophilic performance and excellent water selective performance [105,106], which is very beneficial to remove the

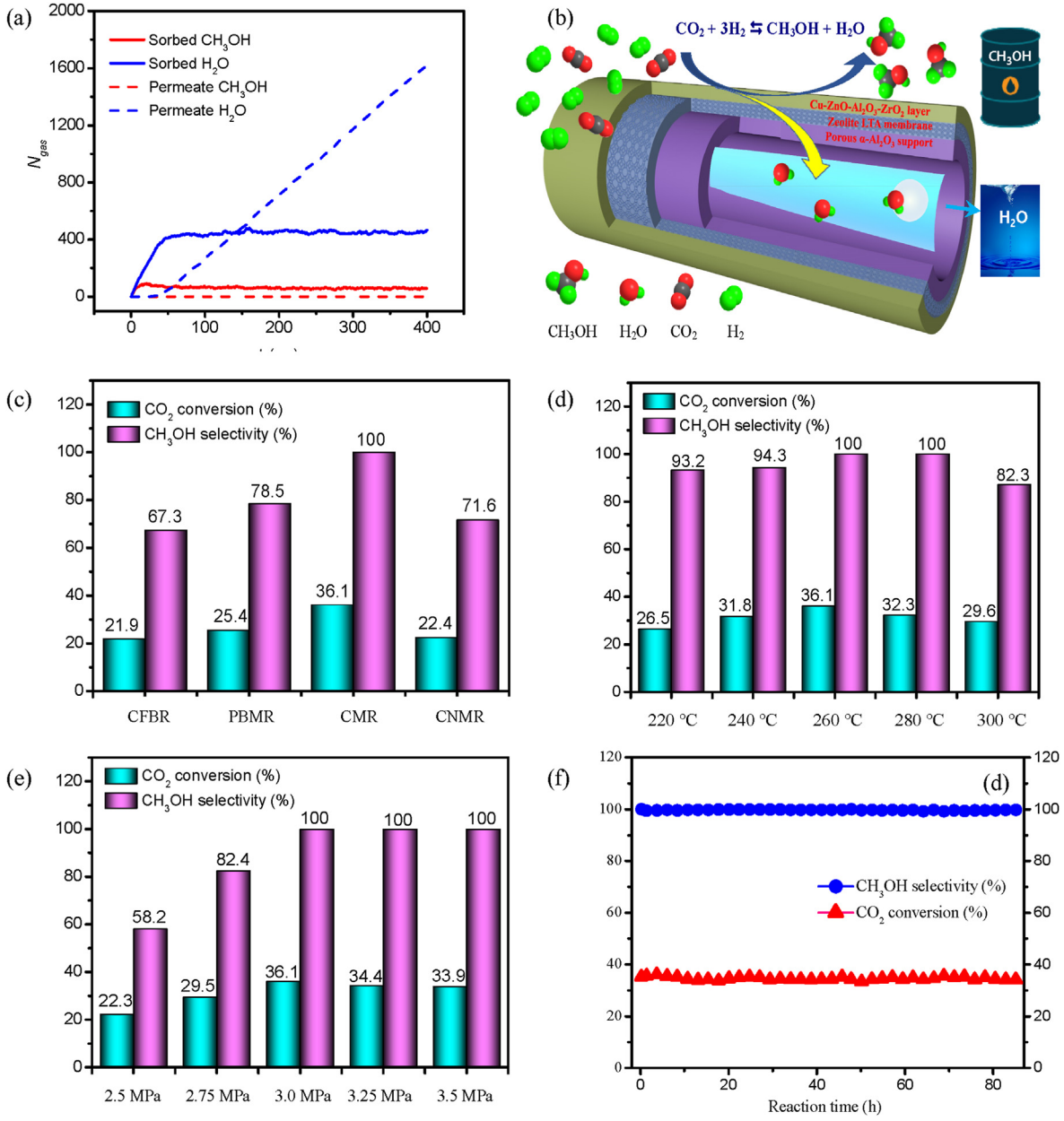

Fig. 10. (a) Numbers of H_2O and CH_3OH molecules sorbed in and permeated through the membrane versus time for the gas mixture at a total pressure of 3 MPa. (b) Scheme of CO_2 hydrogenation to methanol through in-situ and continuous removal of water in a reaction-separation bi-functional LTA@Cu–ZnO–Al_2O_3–ZrO_2 catalytic membrane reactor (CMR). (c) Catalytic performances of the catalytic membrane reactor (CMR) in the CO_2 hydrogenation to methanol in comparison with catalytic fixed bed reactor (CFBR), packed bed membrane reactor (PBMR), and catalytic non-permselective membrane reactor (CNMR). Catalytic performances of CO_2 hydrogenation to methanol in CMR as functions of reaction temperatures at 3.0 MPa (d), reaction pressures at 260 °C (e), and operation time at 260 °C and 3.0 MPa (f). H_2/CO_2 ratio of 3 in the feed, GHSV of 3000 h^{-1}. Reprint from Ref. [16].

by-product water produced during CO_2 hydrogenation to methanol, thus improving the conversion of CO_2 and selectivity of methanol [16,104]. Zeolite LTA membranes are usually prepared on the porous substrates by simple in-situ hydrothermal synthesis. However, due to poor nucleation and robust negative surface charge of LTA building blocks, the LTA layer often contain inter-crystalline defects [107]. So far, various methods, such as secondary growth with seeds [108], multi-stage synthesis [109], synthesis in the microwave field [110], centrifugal force field [111] or electric field [112], have been developed to improve the membrane growth. Huang and colleagues have developed a novel seeding-free synthesis tactics to accelerate the nucleation and crystal growth of zeolite LTA membranes. With covalent modification of the porous substrates by using 3-aminopropyltriethoxysilane [113], 1, 4-diisocyanate [114], 3-chloropropyltrimethoxysilane [115], or polydopamine [116], covalent linkers between the LTA layer and the porous substrates can be formed to adsorb and anchor the zeolite precursors, thus significantly enhancing the nucleation and growth of zeolite layers.

3.3. *Design and fabrication of CMRs for utilization of CO_2*

The design of CMRs needs to consider how to realize perfect combination of reaction and separation. Yu and coworkers reported hydrogenation of $CO_2$to methanol via a packed bed membrane reactor [3], in which the Cu–ZnO–Al_2O_3 catalyst was packed onto the surface of NaA membrane. The NaA membrane has an accurate water-conducting nano-channel based on the gating effect of Na^+, which can allow water

effectively pass through, while gases such as H_2, CO and CO_2 can't pass through (Fig. 9). The by-product steam of the reaction was removed by the NaA membrane, contributing to obvious intensification of the CO_2 conversion (~60%) and methanol selectivity (~70%). Recently, Huang and colleagues have developed a reaction-separation dual-functional CZAZ@LTA membrane reactor for catalytic hydrogenation of CO_2 to methanol [16]. In the prepared catalytic membrane reactor, hydrophilic zeolite LTA membrane was used as a selective dehydration separator, and CZAZ catalyst layer was packed on the surface of LTA membrane. The by-product water could be quickly separated from the reactor through the LTA membrane, which was beneficial to overcome the thermodynamic equilibrium of the reaction and promote the reaction towards methanol production, thus significantly enhancing the CO_2 conversion (Fig. 10). In addition, the removal of water from the reactor is in favor of preventing deactivation of catalyst and formation of by-product, thus increasing the selectivity of methanol. Under the reaction conditions of 3.0 MPa and 260 °C, the conversion of CO_2 increased from 21.9% of the fixed-bed reaction to 36.1% of the membrane catalysis reaction, and the methanol selectivity increased from 67.3% of the fixed-bed reaction to 100% of the membrane catalysis reaction. Further, it should be pointed out that in the current CMRs, the catalyst is usually filled in the separation membrane or the catalyst precursor is loaded on the surface of the separation membrane by impregnation method, and then the catalytic membrane is obtained by high-temperature pyrolysis. The catalytic membrane prepared by impregnation-high temperature pyrolysis usually has a weak binding force with the separation membrane, which affects the mechanical stability of the catalytic layer. Moreover, the catalyst prepared by coprecipitation method is easy to cause the aggregation of metal nanoparticles, thus reducing the activity of the catalyst. Therefore, it is still a great challenge to develop a membrane reactor with high catalytic performance for CO_2 catalytic hydrogenation to methanol.

Significant progress has been achieved in the past decades in the preparation of high permselective zeolite membranes, which offers new opportunities to fabricate CMRs. The latest developments in high-performance zeolite membranes have opened a major breakthrough for CO_2 methanolization in a membrane reactor and raised great hope for future success. The introduction of a highly water-permselective LTA zeolite membrane breaks through the reaction thermodynamic equilibrium, the single-pass CO_2 conversion exceeded 60%, and the methanol selectivity was close to 100% [16]. Until now, however, membrane materials that can be used for CO_2 catalytic hydrogenation are still scarce, and it is critical to develop highly water/gas-selective membranes that are resistant to high temperatures and pressure in the presence of water steam.

Moreover, more efforts should be made to address high-efficiency catalytic membrane configurations, sealing problems, long-term stability, and safety issues. The reactor configuration greatly affects the reaction performance, coupling process and manufacturing cost, which is very important for industrial applications. But it is rarely mentioned, and in the future it is necessary to optimize the reactor design to make CO_2 hydrogenation economically feasible and safe. The reactor configurations mainly include hollow fiber, tube and monolith. It is well known that the hollow fiber has a high packing density, but its low mechanical strength makes it difficult in sealing and withstanding high-pressure conditions. The tubular ceramic supported membrane has good mechanical strength that can be well sealed using graphite gasket. The monolith ceramic supported membrane owns superior mechanical strength and high packing density that can be a promising configuration for CMRs. It also has great advantages such as largely reduced sealing points, making it easier in sealing compared with the ceramic hollow fiber and tubular ones.

4. CMRs for hydrogen production

Hydrogen demand has increased continuously in recent years, since the utilization of hydrogen as an energy source can revolutionize issues related to transportation system, energy security, and global climate change, which has motivated researches into developing methods for hydrogen production and separation [117,118]. Currently, a few methods such as water gas shift reaction ($CO + H_2O \rightarrow CO_2 + H_2$), steam reforming of natural gas ($CH_4 + H_2O \rightarrow CO + 3H_2$), and methane partial oxidation ($CH_4 + 1/2O_2 \rightarrow CO + 2H_2$) et al. were employed to produce hydrogen. However, the production of hydrogen associates with many byproducts, and hydrogen purification techniques such as pressure swing adsorption and cryogenic distillation processes are commercially available but energy intensive [119]. Membrane separation process is considered as an attractive alternative depending on the possibility to shift the equilibrium towards hydrogen production, which consumes lower energy as compared to traditional hydrogen purification techniques such as pressure swing adsorption and cryogenic distillation processes [120–122]. Hydrogen production processes with catalytic ceramic membranes can not only produce clean energy source but also consume lower energy, which can indirectly reduce the emission of CO_2 and realize the goal of carbon peaking. Here we focus on membrane materials and catalysts utilized in CMRs and survey recent developments of hydrogen production processes with catalytic ceramic membranes.

4.1. Preparation of membrane materials for hydrogen production

To date, various membrane materials have been explored for hydrogen production processes. Inorganic membranes exhibit high flux performance and superior chemical and thermal stability, which warrant their potential applications for hydrogen production and separation at high temperatures. Three main groups, including (i) dense metallic membranes, (ii) proton conducting ceramic membranes, and (iii) mix ionic-electronic conducting membranes can be classified. Highly pure hydrogen can be produced using dense metallic membranes, particularly those composed of palladium and its alloys. Despite the intensive development and research efforts, the commercial availability of Pd-based membranes is still limited due to their high sensitivity to some gases including HS and CO. As a result, there is a desire for ceramic membranes that are resistant to toxic gases, which would be helpful due to their inert nature.

4.1.1. Palladium membranes

Dense metallic membranes especially pure palladium (Pd) and its different alloys have been widely studied for separation of hydrogen due to their excellent diffusive properties resulting in a highly pure hydrogen (≥99.9999%) [120]. The hydrogen permeation through the membrane is governed by the solution-diffusion mechanism [121,122], i.e., after adsorption on one side of the membrane, the hydrogen molecules dissociate into atoms, transport through the metal matrix, and recombine and desorb on the other permeate side. H_2 can be separated from gas mixtures containing CO, H_2O, CH_4, and other gases by combing Pd-based membranes with catalysts in membrane reactors, and the operating temperatures are between 300~550 °C [123–126]. Tokyo Gas employed Pd membrane reformer and developed the world's highest efficiency (81.4%) of H_2 production from natural gas with the largest H_2 production rated capacity (40 N m^3/h) [127]. However, pure Pd membranes suffer from embrittlement, poisoning, and phase transition under H_2 exposure since hydrogen is likely to be frozen in the Pd lattice. These harmful effects can be evaded by alloying palladium with other metals, including Ag [128,129], Cu [130,131], Au [130,132], Ru [133,134] et al. These Pd alloys revealed higher catalytic performance for H_2 dissociation and recombination as compared with pure Pd. Fernandez et al. investigated Pd–Ag membranes for H_2 separation and reported high permselectivity of H_2 and N_2 (>200,000) at the temperatures of 400–673 °C [128]. Sonwane et al. investigated the diffusivity of H_2 in Pd-based membranes using density functional theory (DFT) and demonstrated 10 times increase in H_2 solubility at 183 °C for the $Pd_{70}Ag_{30}$ membrane as compared with pure Pd [129]. Jia et al. studied the thermal stability of Pd–Cu and Pd–Au alloy membranes, and indicated that the ability of Pd–Cu

membranes was maintained up to 650 °C, whereas the deterioration occurred at 550 °C for Pd–Au membranes [130]. In spite of the significant research and development efforts, palladium membranes show problems in terms of poisoning of the membrane surface and reduction of the effective H_2 fluxes by 20% up to 100%, due to their acute susceptibility to chemicals such as carbon monoxide, chlorine, and sulfur. Their commercial availability is therefore still restricted.

4.1.2. Proton conducting ceramic membranes

In the cases of dense ceramic membranes, hydrogen transports via the coupled permeation of electrons or electron holes and protons, and this permeation of hydrogen is thus dependent on the conductivities of the electronic species and the protons, which is different from that in metallic membrane cases. In this regard, the dense ceramic membranes potentially offer 100% H_2 selectivity when they are defect-free, with mechanical and chemical stability at the operating temperatures between 500 and 900 °C. Mixed protonic-electronic conducting (MPEC) ceramic materials with perovskite structures have been recognized as potential candidates for H_2 separation and production membranes [135,136]. The phenomenon that doped $SrCeO_3$ perovskite oxides has high protonic conductivity was first discovered by Iwahara et al. [137] in a hydrogen-containing atmosphere at high temperatures (>500 °C), followed by the intensive studies of perovskite-based oxide ceramic materials ($SrCeO_3$, $BaCeO_3$ and $BaZrO_3$) [138,139]. Unfortunately, these kinds of materials show low (less than 0.03 mL cm^{-2} min^{-1}) hydrogen permeability, and doping strategies were thus adopted to intensify the mixed protonic-electronic conductivity that related with the H_2 permeation properties. Compared with the undoped $SrCeO_3$ and $BaCeO_3$, $BaCe_{1-x}M_xO_{3-\delta}$ and $SrCe_{1-x}M_xO_{3-\delta}$ (M = Nd, Tm, Eu, Tb, Yb, Sm etc.) exhibited improved electronic conduction upon doping/substitution with M-cations with mixed valence [140–143]. Malavasi et al. [144] studied the role of preparation route on the transport performance of $BaCe_{1-x}Y_xO_{3-\delta}$ and reported high proton conductivity (10^{-2} Ω^{-1} cm^{-1} at 600 °C) when 15% or 20% of Y was incorporated. Wang et al. [145] proposed a $La_{5.5}(W_{0.6}Mo_{0.4})_{0.95}Pd_{0.05}O_{11.25-\delta}$ membrane using an efficient in-situ exsolution strategy. Pd nanoparticles were in-situ generated and dispersed uniformly on the membrane surface, which greatly promoted the H_2 surface exchange kinetics and subsequently increased the H_2 permeation flux (1.3 mL cm^{-2} min^{-1}, 1000 °C).

Despite significant strides made in developing single phase MPEC membranes, the main challenge with respect to find materials with high proton and electronic conductivities simultaneously. An alternative approach is to combine two separate materials, one with high proton conductivity and another with high electronic conductivity; forming the so-called composite membranes or dual-phase such as ceramic-ceramic and ceramic-metallic membranes. The metal incorporation with Ni, Ag, Pd, Au, and Pt etc. intensifies the interfacial catalytic activities and increases the electronic conductivity of the MPEC membranes [146–149]. Lee et al. [147] investigated the hydrogen-separation properties of Ni–$BaCe_{0.9}Y_{0.1}O_{3-\delta}$ (Ni-BCY) membrane, containing Ni as the electronic-conducting metal phase and BCY as the proton-conducting ceramic phase. The hydrogen permeability could be significantly improved so that a H_2 flux of 0.76 mL cm^{-2} min^{-1} at 800 °C was achieved. This improved hydrogen permeation could be attributed to the occupation of transition metal cation in B-site crystal lattice position, enhancing the electronic conductivity with high proton conductivity retained. However, its electronic conductivity was generally lower than ionic conductivity. Rare earth-doped ceria oxides (such as $Ce_{0.8}Y_{0.2}O_{2-\delta}$ and $Ce_{0.85}Gd_{0.15}O_{2-\delta}$) are known to exhibit exceptional n-type electronic conductivity in a reducing atmosphere at temperatures exceeding 600 °C due to the reduction of Ce^{4+} to Ce^{3+}. In order to guarantee efficient electronic transport across the H_2 separation membrane under high temperatures and reducing atmospheres, the addition of doped ceria to barium cerate or cerate-zirconate above the percolation extremity is necessary. Rebollo et al. prepared a dual-phase membrane consisting of $BaCe_{0.65}Zr_{0.2}Y_{0.15}O_{3-\delta}$ and $Ce_{0.85}Gd_{0.15}O_{2-\delta}$. The hydrogen showed an increase in flux to 1.75 mL cm^{-2} min^{-1} and 2.40 mL cm^{-2} min^{-1} at a temperature of 1040 °C. This increase was observed when both membrane sides and only the sweep side were hydrated, respectively [150]. These H_2 fluxes values are presently among the highest recorded for bulk mixed protonic-electronic membranes. In order to avoid the occurrence of new miscellaneous phases resulting from the diffusion of cations between distinct ceramic phases at elevated temperatures, a novel concept of automatic phase separation has been put forward and employed in synthesizing a dual-phase ceramic membrane by Wang et al. [151]. At a temperature of 950 °C, the dual-phase membrane $BaCe_{0.85}Fe_{0.15}O_{3-\delta}$-$BaCe_{0.15}Fe_{0.85}O_{3-\delta}$ with 1.0mm thickness showed an exceptionally high H_2 permeation flux of 0.76 mL cm^{-2} min^{-1} and good chemical compatibility.

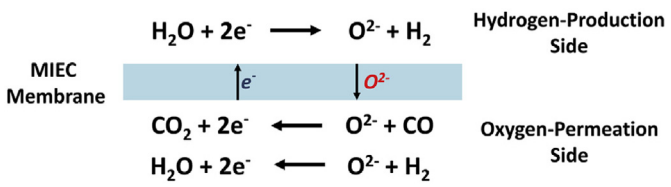

Fig. 11. Schematic diagram for the hydrogen production from water splitting in MIEC membrane reactor.

4.1.3. Mix ionic-electronic conducting membranes

Mixed ionic-electronic conducting (MIEC) membranes are a kind of oxidic dense ceramic membranes that can conduct oxygen ions and electrons simultaneously. When there is an established oxygen partial pressure gradient across the MIEC membrane, the oxygen permeation mechanism can be described as, oxygen ion undergoes migration from a region with high oxygen partial pressure towards another area with low oxygen partial pressure [152], that is to say, only oxygen can transport though the membrane. Fig. 11 depicts the fundamental principle of hydrogen generation within the MIEC membrane reactor, taking water splitting reaction for an example. Water splits into hydrogen and oxygen at the hydrogen-production side at high temperature, meanwhile the oxygen-permeation membrane side is swept by reducing gases, such as methane [153], synthesis gas [17], low-purity hydrogen [154], which react with the oxygen that permeates from the hydrogen-production membrane side. In this sense, oxygen ions are driven to transport persistently from the hydrogen-production side to the oxygen-permeation side as an oxygen chemical potential ramp is established across the membrane. As a result, 100% of hydrogen purity is obtained after cooling and drying from the hydrogen-production membrane side. Owning to the ability of producing pure hydrogen without the need for electric power, the MIEC membrane technology for hydrogen production has gained global attention. The rate of hydrogen production is directly influenced by the oxygen permeability of membranes, MIEC membranes exhibiting high oxygen ionic conductivities and electronic are therefore expected.

Naito and Arashi [155] studied hydrogen production in a MIEC ZrO_2–TiO_2–Y_2O_3 membrane reactor in the early work, and reported a 0.6 mL cm^{-2} min^{-1} hydrogen production rate at high temperature of 1683 °C. The membrane material with low electronic conductivity limited the hydrogen production rete in this case. Recently, some new membrane materials were investigated to improve the hydrogen production rate and lower the operation temperature, which can be classed into (i) perovskite-based membranes and (ii) dual-phase fluorite-perovskite composite membranes. Perovskite materials ($ABO_{3-\delta}$) containing Co or Fe in the B site are considered having high oxygen permeability. Balachandran et al. [40] investigated a $La_{0.7}Sr_{0.3}Cu_{0.2}Fe_{0.8}O_{3-\delta}$ (LSCF) perovskite membrane for hydrogen production from water splitting reaction, and a hydrogen production rate of 4.7 mL cm^{-2} min^{-1} was achieved at 900 °C when 99.5% CO was fed to the oxygen permeation side and water vapor to the hydrogen-production side. After that, perovskite

materials, such as $SrCo_{0.4}Fe_{0.5}Zr_{0.1}O_{3-\delta}$ [156], $BaZr_xCo_yFe_zO_{3-\delta}$ [157, 158], were explored for hydrogen production. Yang et al. [42] innovatively employed a $Ba_{0.98}Ce_{0.05}Fe_{0.95}O_{3-\delta}$ membrane in the membrane reactor to separate hydrogen via the water splitting reaction. They obtained appropriate proportions ($H_2/N_2 = 3$) of ammonia syngas of 18.8 mL cm^{-2} min^{-1} and liquid fuel gas of 45.6 mL cm^{-2} min^{-1} at 925 °C. Compared with the industrial production processes, the MIEC membrane technology can save 63% energy consumption and is promising for industrial applications [159]. However, the current perovskite materials containing iron or cobalt exhibit limited tolerance to reduction, development of Co- or Fe-free perovskite membranes are necessary. He et al. [160] reported for the first time the $SrMg_{0.15}Zr_{0.05}Ti_{0.8}O_{3-\delta}$ membrane that exhibited enhanced reduction tolerance in 20 vol% H_2/Ar for 100 h, and further demonstrated that the hydrogen and synthesis gas could be simultaneously obtained by coupling methane reforming and water splitting.

In order to enhance the stability of MIEC membranes, which is more important for commercialization of membrane technologies than permeability, fluorite-perovskite dual-phase membrane materials were explored. Pal et al. [161] investigated hydrogen production performance using a fluorite-perovskite dual-phase membrane composed 60 vol% $Gd_{0.2}Ce_{0.8}O_{2-\delta}$ (GDC) as an oxygen ionic conductor and 40 vol% $Gd_{0.08}Sr_{0.88}Ti_{0.95}Al_{0.05}O_{3\pm\delta}$ (GSTA) as a n-type electronic conductor. This material showed a hydrogen production rate of 9.67 mL cm^{-2} min^{-1} at 900 °C and excellent chemical stability in operating conditions compared to the corresponding single-phase perovskite membranes, such as $La_{1-x}Ca_xFeO_{3-\delta}$ [162] and $La_{1-x}Sr_xCo_yFe_{1-y}O_{3-\delta}$ [161]. Recently, Jiang et al. [48] developed a Ti-based dual-phase membrane material consisting $Ce_{0.9}Pr_{0.1}O_{2-\delta}$-$Pr_{0.1}Sr_{0.9}Mg_{0.1}Ti_{0.9}O_{3-\delta}$, which displayed excellent structural and thermal stabilities and at a temperature of 940 °C achieved a stable H_2 production rate of 0.52 mL cm^{-2} min^{-1} for 180 h. The surface modification can further improve the production rate of hydrogen. Therefore, it is necessary to exploit membrane materials with excellent stability and good oxygen permeability in reducing conditions to realize their applications for hydrogen production.

4.2. Design and fabrication of CMRs for hydrogen production

4.2.1. Steam methane reforming (SMR)

Methane containing gaseous fuels such as natural gas, shale gas or biogas is currently economical source for hydrogen production. Steam methane reforming (SMR, $CH_4 + H_2O \rightarrow CO + 3H_2$) has been extensively applied for hydrogen or syngas production [163]. Generally, the produced syngas has a high H_2/CO ratio of up to 3, which is detrimental for the Fischer-Tropsch or methanol synthesis. Thus, the H_2/CO ratio should be adjusted to 2 [164]. Additionally, the syngas can go through a WGS reaction to produce hydrogen [165]. However, it is worth noting that H_2 production through WGS may result in the presence of poisonous CO residue, which can negatively impact Pt electrocatalysts in fuel cells. Xia et al. [166] presented a novel method of linking SMR with H_2 removal in a proton conducting membrane reactor (50 mol% $BaCe_{0.85}Fe_{0.15}O_{3-\delta}$-50 mol% $BaCe_{0.15}Fe_{0.85}O_{3-\delta}$) to collaboratively manufacture CO-free H_2 and syngas with a preferable H_2/CO ratio of 2 on the opposite sides of the membrane, which will facilitate direct use for the Fischer-Tropsch synthesis and fuel cells, respectively.

4.2.2. Partial oxidation of methane (POM)

Currently, partial oxidation of methane (POM, $CH_4 + O_2 \rightarrow CO + 2H_2$) with pure oxygen is regarded as the most promising method for CH_4 conversion due to high selectivity to syngas, good exothermicity, and high CO/H_2 ratio. The CMRs based on MIEC membranes can integrate air separation with POM reaction in a single unit, and oxygen species are constantly supplied via the membrane to react with methane, thereby preventing deep oxidation of products and resulting in a 30% reduction in capital costs. This cutting-edge technology is expected to revolutionize the chemical and petroleum industries [167].

Compared to the membrane reactors without addition of catalysts, the CMRs with the integration of catalysts and ceramic-based membranes show better performance [168–170]. The Ni-based CMR shows superior conversion and activity. To prevent agglomeration of Ni and maintain a small particle size at high temperatures, strong metal-support interaction is necessary. Jiang et al. demonstrated a $Ba_{0.5}Co_{0.5}Fe_{0.22}Nb_{0.08}O_{3-\delta}$ four-channel hollow fiber catalytic membrane reactor coated with in-situ exsolved $FeNi_3$ nano-catalyst $Sr_{0.9}(Fe_{0.81}Ta_{0.09}Ni_{0.1})O_{3-\delta}$ for POM [171]. The conversion of methane, selectivity of carbon monoxide and hydrogen were 98%, 97% and 98%, respectively. Wang et al. reported a $BaBi_{0.05}Co_{0.8}Nb_{0.15}O_{3-\delta}$ (BBCN) perovskite-type hollow fiber membrane coated with Ni phyllosilicate catalyst for POM at low temperatures (650–750 °C) [172]. At 730 °C, the 80%conversion of methane and 85% selectivity of CO were achieved. Tsai et al. explored POM in a $La_{0.2}Ba_{0.8}Fe_{0.8}Co_{0.2}O_{3-\delta}$ ceramic membrane reactor [173]. The methane conversion of 78% and oxygen permeation rate of 4.2 mL cm^{-2}·min^{-1} were realized. Compared with membrane reactors without catalysts, the oxygen permeation rate was 5 times higher and the methane conversion was 4 times higher in a membrane reactor with 5%Ni/Al_2O_3 catalyst. Although the membrane reactor operated stably for 850 h, the morphology, surface structure and element composition of the membrane were significantly changed, because the contact of the membrane with CO and H_2 from POM caused the lost lattice oxygen of perovskite oxide. Therefore, choosing appropriate membrane materials is also pivotal for maintaining stable performance under long-term reducing gas environments in POM. In general, the thermal and chemical stability of membranes can be improved by reducing the amount of cobalt doping, doping anti-reduction metal ions such as Ce^{4+} [174], Zr^{4+} [175], Ti^{4+} [46], Ga^{3+} [176], Al^{3+} [177] and Zn^{2+} [178] in the B-site of perovskite, and developing cobalt-free materials.

4.2.3. H_2O splitting

Hydrogen production technology with water as hydrogen source demonstrates a good application scenario because of its cleanliness and reproducibility. Although water decomposition into oxygen and hydrogen ($H_2O \rightarrow H_2 + 1/2O_2$) is conceptually simple, the efficient hydrogen production from water remains a long-standing challenge due to a low equilibrium constant of 2×10^{-8} at 950 °C [179]. The application of MIEC membranes in water splitting for hydrogen production enables simultaneously removal of oxygen and acceleration of H_2 production rate. Hydrogen production in CMRs based on oxygen-permeable membranes coupling water splitting with some heterogeneous reactions, including the oxidative coupling of hydrocarbon, partial oxidation of hydrocarbon, and oxidative dehydrogenation of hydrocarbon, has attracted extensive research interest due to its distinct advantages of 100% O_2 selectivity and process intensification [180]. Jiang et al. first conducted research on water splitting (WS) coupling POM in a $BaCo_xFe_yZr_{1-x-y}O_{3-\delta}$ (BCFZ) hollow fiber membrane packed with Ni-based catalysts in POM reaction side [15]. The synthesis gas and hydrogen was manufactured simultaneously. The H_2 production rate of 3.1 mL cm^{-2} min^{-1}, CH_4 conversion of 70% and CO selectivity of 60% were achieved at 950 °C. In addition, Jiang et al. combined WS with oxidative dehydrogenation of ethane to ethylene in a $BaCo_xFe_yZr_{1-x-y}O_{3-\delta}$ (BCFZ) hollow fiber membrane to produce ethylene and hydrogen [167]. On the core side of the membrane, the water dissociated into hydrogen and oxygen occurred. The generated oxygen was subsequently removed as oxygen ions to the shell side and reacted with ethane to yield water and ethylene. At 800 °C, a rate of hydrogen production about 1.0 mLcm^{-2} min^{-1} was achieved alongside an ethylene yield of around 53%. Beyond that, oxidative steam reforming of ethanol (OSRE) is also promising in producing hydrogen. Among the various ethanol reforming routes for H_2 production, OSRE is an attractive option ($C_2H_5OH + 2H_2O + 1/2O_2 \rightarrow 2CO_2 + 5H_2$). Zhu et al. developed a highly effective and sustainable route for H_2 production, which combined WS with OSRE in a tubular $SrCo_{0.4}Fe_{0.5}Zr_{0.1}O_{3-\delta}$ membrane reactor packed with Ni/Al_2O_3 [156]. At 750 °C, the hydrogen production rates of 6.8 and 1.8 mL cm^{-2} min^{-1},

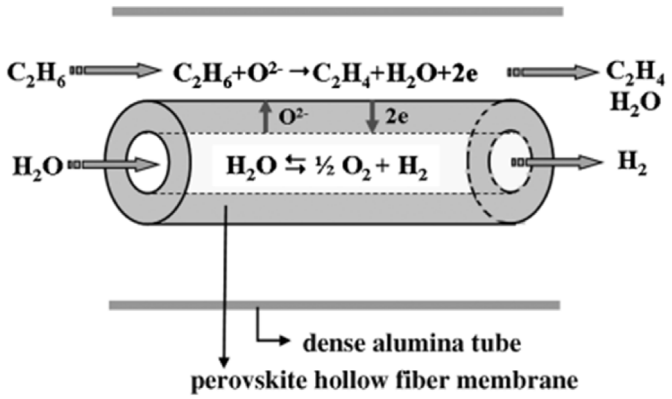

Fig. 12. Schematic diagram of membrane reactor for combining water splitting with ethane dehydrogenation. Reprint from Ref. [156].

respectively, were achieved by coupling OSRE at the shell side with WS reaction on the opposite sides of the oxygen permeable membrane (Fig. 12). In addition, Morejudo et al. showed that the integration of an electrochemical $BaZrO_{3-\delta}$ membrane exhibiting both oxide ion conductivity and proton into nonoxidative methane dehydroaromatization (MDA: $6CH_4 \leftrightarrow C_6H_6 + 9H_2$) reactor leads to elevated levels of aromatics production and enhanced durability of the catalyst [181].

4.2.4. Other CMRS for hydrogen production

The methane dry reforming (DRM) reaction ($CH_4 + CO_2 \rightarrow 2CO + 2H_2$) is an efficient and environmentally friendly strategy to achieve simultaneous greenhouse gas conversion to reduce carbon footprints and syngas production and utilize natural gas and biogas that contains abundant CO_2 [182]. DRM is a violently endothermic reaction, and a theoretical ratio of CH_4 and CO_2 of 1:1 is required. However, the concentration of CO_2 in biogas is less than CH_4 concentration, making it very difficult to prevent the coke deposition. Therefore, it is proposed that the DRM can combine with the exothermic partial oxidation of methane in a CMR to realize total conversion of methane into syngas and alleviate the carbon deposition. He et al. developed a dual-phase $Ce_{0.9}Gd_{0.1}O_{2-\delta}$-$Gd_{0.1}Sr_{0.9}Fe_{0.9}Ti_{0.1}O_{3-\delta}$ disk membrane reactor to couple air separation with biogas reforming [183]. After operation at 890 °C for 150 h, the membrane reactor could still sustain high methane conversion of 83%, high CO selectivity of nearly 100% and high oxygen permeability of 1.1 mL cm^{-2} min^{-1}.

Benefiting from the in-situ oxygen removal by the membranes, effective co-conversion of CO_2 and H_2O into syngas can be achieved at relatively lower temperatures (<1000 °C). Liang et al. employed a $Ce_{0.9}Pr_{0.1}O_{2-\delta}$-$Pr_{0.6}Sr_{0.4}FeO_3$ MIEC membrane reactor for the co-conversion of CO_2 and H_2O into syngas, and in the opposite side, the methane was utilized to accelerate both oxygen permeation and produce syngas [184]. Under the circumstances, high-temperature furnace was utilized as a substitution of solar oven. At 930 °C, 1.3 mL cm^{-2} min^{-1} syngas production rate was achieved in the H_2O/CO_2 co-feeding side. Meanwhile, the CH_4 conversion of 62%, CO selectivity of 99% and corresponding syngas production rate of 3.9 mL cm^{-2} min^{-1} were achieved.

5. CMRs for efficient liquid-phase hydrogenation

Hydrogenation is a crucial process in the chemical, petrochemical, and fine chemical industries [5]. Traditional hydrogenation reactors have some limitations, such as poor heat transfer, serious back-mixing of reactants and difficult separation of catalysts. Loading active components on the membranes and then constructing CMRs can enhance the contact between the reactants and active components, reducing the mass transfer limitation. Furthermore, CMRs can control the flow of reactants, decreasing their back-mixing. Additionally, there is no need to separate catalytic materials from the reaction system, thereby enhancing the process efficiency. CMRs have been employed in the gas phase hydrogenation such as CO_2 to CO to C1–C2. Recently, there are some reviews on the topic [30,60,185,186]. And, CMRs for the gas phase hydrogenation of CO_2 to methanol are reviewed in section 3. Hence, CMRs applied in the gas-phase hydrogenation will not be discussed in this section, and the section focuses on reviewing the progress of catalytic membranes in liquid-phase hydrogenation.

5.1. Synthesis of catalytic membranes for liquid-phase hydrogenation

The catalytic membrane is a crucial component of the membrane reactor, and its performance directly impacts the efficiency of membrane reactor. The preparation of catalytic membranes mainly involves the preparation of membranes [187], the modification of membrane surface [18,188], and the introduction of active components [18,188]. Active components are frequently loaded via various techniques such as impregnation [18], atomic layer deposition [188], and chemical vapor deposition [189]. Many efforts have been made to create high-efficiency catalytic membranes for liquid-phase hydrogenation.

5.1.1. Configurations of catalytic membranes

The configuration of the membrane has significantly influence on the membrane area per unit volume, a crucial determinant of capacity of loading active components [5]. The membrane configurations are primarily classified as flat-sheet [18], tubular [189], hollow fiber [12], and nanofiber [13].

Miao et al. [18] modified the flat-sheet ceramic membrane by loading branched TiO_2 nanorods. This modification significantly increased the surface area from 0.16 to 1.45 m^2/g, resulting in a three-fold increase in the Pd content and a 1.6-fold increase in the initial hydrogenation rate of *p*-nitrophenol for the catalytic membrane. Peng et al. [190] applied ZnO nanoparticles (NPs) to modify the surface and pores of a tubular ceramic membrane, followed by impregnating Pd onto the modified ceramic membrane. XPS and HRTEM results confirmed the formation of an alloy between Pd and Zn. The resulting catalytic membrane exhibited excellent stability in the liquid-phase hydrogenation of *p*-nitrophenol. Chen et al. [12] synthesized a Pd/hollow fiber ceramic catalytic membrane by loading Pd onto a hollow fiber ceramic membrane. The hollow fiber structure provided a larger surface area for the deposition of Pd NPs compared to a single-tube ceramic membrane of equivalent volume, resulting in a higher catalytic activity for the hydrogenation of *p*-nitrophenol (44% increase in the hydrogenation rate).

In recent years, it is found that the nanofiber membranes have extensive applications in catalysis due to their stable porous structures, high porosity, and large specific surface areas, which significantly improve the membrane flux and lower the mass transfer resistance [13]. Zhu et al. [13] grew UiO-66-NH_2 NPs on the SiO_2 fiber membrane by a solvent thermal method, and then loaded Pd to produce a hierarchically porous Pd/UiO-SiO_2 catalytic membrane. Due to the developed hierarchically porous structure, high specific surface area, and high Pd loading, the excellent catalytic activity and stability were obtained.

The membrane area per unit volume of sheet and single-tube membranes is relatively low, which limits the content of active components per unit volume of catalytic membranes. Hollow fiber and nanofiber membranes offer a larger surface area per unit volume and can accommodate a greater loading of active components, resulting in enhanced catalytic activity [12]. However, the fiber membranes, while possessing certain benefits for catalytic hydrogenation, have limited mechanical strength and lack well-developed processes for large-scale preparation and module fabrication. Consequently, up to date, the efficiency of the catalytic membranes is not competitive as compared to powder catalysts, with the researches remaining primarily in the laboratory stage. The multi-channel ceramic membrane emerges as a more viable alternative with its considerable mechanical strength, ample surface area per unit volume, and greater maturity in the module fabrication. Given these advantages, the fabrication of a multi-channel ceramic catalytic

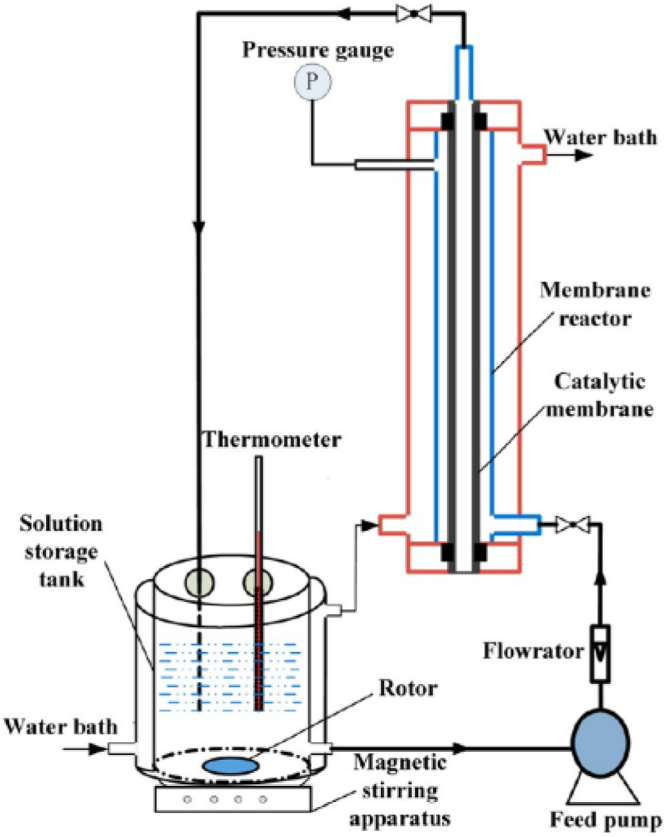

Fig. 13. Experimental setup for the preparation of a Pd catalytic membrane with a flow-through method. Reprint from Ref. [193].

membrane presents itself with substantial potential for high-efficiency hydrogenation applications.

5.1.2. *Methods for loading active components*

The hydrogenation capacity of a catalytic membrane is primarily limited by the amount and distribution of the active component. The method of loading has a substantial impact on the both factors. To date, many methods have been developed for loading active components, such as impregnation [191], layer-by-layer deposition [192], chemical vapor deposition [189], sol-gel [193], electroless deposition [194], flow-through [193] and atomic layer deposition [188].

Zhou et al. [195] employed the impregnation method to synthesize a Pd/α-Al_2O_3 catalytic membrane. In this approach, a palladium chloride emulsion was added to a microemulsion containing a reducing agent under nitrogen atmosphere via a peristaltic pump. The tubular ceramic membrane was then immersed in the microemulsion containing Pd NPs, with ethanol solution gradually added to reduce the stability of the microemulsion system. This resulted in Pd NPs being gradually deposited onto the surface and pores of the tubular ceramic membrane. After impregnation, the tubular membrane was calcined in air atmosphere to obtain the Pd/α-Al_2O_3 catalytic membrane. In the selective hydrogenation of 1,5-cyclooctadiene, the activity and selectivity of Pd/α-Al_2O_3 catalytic membrane were higher than those of Pd-PAA catalytic membrane. However, the microemulsion employed in the impregnation process was inherently unstable, leading to the aggregation of Pd NPs in the porous membrane. Consequently, the multilayer assembly technique has been developed as a simple and highly effective means of loading active components, allowing for the deposition of high-density metal NPs on a wide variety of carriers [195]. Importantly, the alternate adsorption of layers can be used to adjust the loading amount of metal by carefully modulating the type and number of adsorption layers. As well as preventing the contact and aggregation of metal NPs, this approach serves to enhance the overall catalytic efficiency [196].

The traditional impregnation method has faced numerous challenges, notably the difficulty in overcoming the capillary force in membrane pores, thereby hampering the entry of the impregnation solution containing active components. Unfortunately, this shortcoming implies that the active component of the resultant catalytic membrane is generally loaded on the surface of the membrane, leading to lower catalytic efficiency. To overcome the shortcoming, Li et al. [193] developed a flow-through method to prepare catalytic membranes (as illustrated in Fig. 13). Under the action of the pump, the solution containing Pd was forced through the membrane pores, and the Pd NPs were loaded on the surface and pores of the ceramic membrane. This method increased the Pd loading amount by approximately 47%, in comparison with the traditional impregnation approach. Based on the significant improvement, the Pd catalytic membrane demonstrated superior hydrogenation efficiency toward the *p*-nitrophenol reduction, with a 28% increase in the *p*-nitrophenol conversion, as compared to the Pd catalytic membrane prepared using the impregnation method.

Chen et al. [197] successfully developed a catalytic membrane by exploiting flow synthesis and displacement reaction to embed a Cu-Agx bimetallic catalyst into the pores of the membrane for the hydrogenation of *p*-nitrophenol. Through the regulation of Ag^+ concentration, the degree of spontaneous electrochemical displacement reaction in the flow process could be adjusted to control the proportion of bimetallic components. In the catalytic process, the Cu core acted as an electron-deficient site that adsorbed and activated the $-NO_2$ group of *p*-nitrophenol, while the Ag shell enhanced the overflow of active hydrogen to the Cu surface, where it facilitated the hydrogenation reaction. The catalytic membrane achieved a high apparent reaction rate constant, which generally increased with the Ag content, but eventually decreased with further increase in the Ag content.

Lu et al. [188] deposited the active component Pd on the ceramic membrane through atomic layer deposition (ALD). TiO_2 was also deposited by ALD and subsequently calcined to modify the membrane surface. Adjusting the calcination atmosphere facilitated the control over the surface properties of the ceramic membrane. The catalytic performance of the resulting catalytic membrane in the reduction of *p*-nitrophenol to *p*-aminophenol was observed to be strongly dependent on both the deposition parameters and calcination atmosphere.

5.2. *Design and fabrication of CMRs for liquid-phase hydrogenation*

For liquid-phase hydrogenation, the catalytic membrane not only has

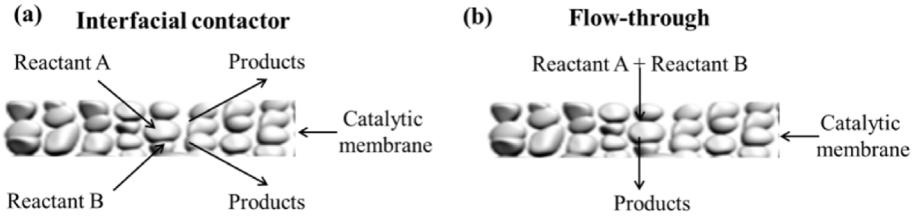

Fig. 14. Schematic diagram of two modes of contactor-type CMRs: (a) Interfacial contactor, (b) Flow-through.

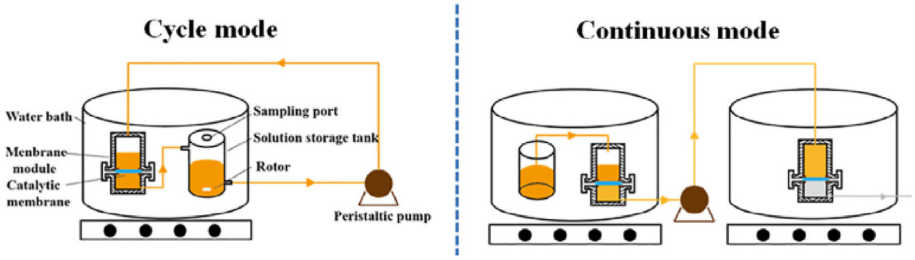

Fig. 15. Experimental setup of a flow-through catalytic membrane reactor. Reprint from Ref. [18].

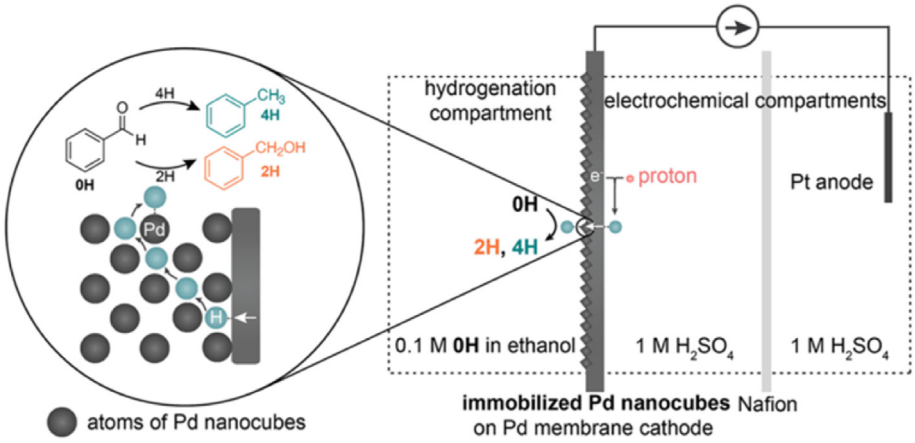

Fig. 16. Schematic diagram of the three-compartment cell for performing hydrogenation with immobilized Pd nanocubes drop-cast on a bare Pd foil. Reprint from Ref. [202].

the catalysis function, but also can serve as the distributor and contactor. Therefore, CMRs for liquid-phase hydrogenation can be mainly divided into distributor-type CMRs and contactor-type CMRs.

Distributor-type CMRs offer the ability to control the reactant concentration by limiting its entry into the reaction zone through the membranes, thus reducing the by-side reactions. Consequently, controlling the addition of hydrogen through distributor-type CMRs can effectively prevent the deep hydrogenation and minimize the by-product generation, thereby providing significant advantages in the selective hydrogenation. Gryaznov and coworkers [2] were pioneers in employing palladium catalytic membranes (including palladium alloy membranes) in the selective hydrogenation of unsaturated hydrocarbons, such as cyclopentadiene, 1,3-pentadiene, and acetylene. Results revealed that the hydrogen molecules through the palladium catalytic membranes were more active than those in the gas or liquid phases.

Contactor-type CMRs can be categorized into two types based on the contact mode (Fig. 14). In the first type, the catalytic membrane serves as an interface for the reactants, and the reactants feed from the two sides of the catalytic membrane (Fig. 14a), thereby significantly reducing the diffusion resistance and enhancing the reaction rate [198]. Unfortunately, the operation mode requires high integrity of the catalytic membrane [14], limiting its applications. In the second type, the reactants are pressured to flow through the pores of the catalytic membrane (Fig. 14b), thereby contacting fully with the active components for the catalytic reaction. This feature boosts the reaction rate and conversion, making it more efficient than the first type and attracting broad attention [199]. Furthermore, the contact time between the reactants and catalytic membrane can be regulated by altering the flow rate of the reactants. Miao et al. designed and constructed a flow-through CMR for the reduction of *p*-nitrophenol (Fig. 15) [18]. Under a continuous flow mode, the conversion of *p*-nitrophenol (at a concentration of 4176 mg/L) to *p*-aminophenol was completed within 24 s in the flow-through CMR. Furthermore, the reactor could operate continuously and stably for up to 240 min.

Generally, the hydrogenation reaction in CMRs requires the introduction of hydrogen sources, such as hydrogen and sodium borohydride, which involves the storage and transportation of hydrogen sources. To address this issue, Iwakura et al. [200–202] developed a selective hydrogen permeation catalytic membrane that enabled the coupling of the electrolytic water reaction and hydrogenation reaction in one CMR (Fig. 16). The hydrogen produced by electrolysis functioned as the active hydrogen species and could be transferred to the hydrogenation reaction zone via the catalytic membrane. This approach organically combines the green hydrogen production process and hydrogenation process, and reduces the cost of hydrogen storage and transportation.

6. Summary and perspectives

CMRs can allow the selective removal of products, avoid the separation procedure of powder catalysts from the reaction mixture, intensify the diffusion of reactants in the catalytic region, couple different reactions in one unit, and have been widely applied in the capture and efficient utilization of carbon dioxide, hydrogen production and efficient liquid-phase hydrogenation. The recent progresses in the CMRs applied in the fields related to carbon peaking and carbon neutrality are summarized. Although a lot of achievements have been obtained in CMRs, they are mainly at the laboratory stage, and more efforts should be devoted to the development of CMRs.

(1) The catalytic performance and separation ability are pivotal factors of the CMRs, which are tremendously affected by membrane materials and catalytic materials. Preparing highly-efficient membrane materials with high conductivity or permeability and efficient catalysts with high catalytic properties toward typical reactions, and coupling them together well are the key to promote the applications of CMRs.

(2) Design and preparation of catalytic membranes in large-scale are challenging. The development of highly automated scale-up preparation systems is a priority. The laws of the scale-up synthesis of catalytic membranes need to be studied in detail. Furthermore, reusable and low-cost raw materials should be taken into account, making these technologies more acceptable to the industrial community.

(3) The configuration of CMRs greatly affects the system operation and reaction performance, and it is necessary to optimize the reactor design to make the CMR system economically feasible and safe. The sealing of membrane modules under harsh reaction conditions is still unsatisfied, and more attentions should be paid. The multiscale modeling and simulation studies should be extended to open the "black box" of combining catalytic and membrane processes, promoting the applications of CMRs.

(4) The stable run of the CMR system is vitally important for its industrial applications. Design and preparation of catalytic membranes with high chemical and structural stability toward typical reactions under operation conditions are required. The operation conditions should be optimized to guarantee the stability of the CMR system. Furthermore, the in-situ characterization means can be introduced to make the evolution of catalytic membranes more clear, and thus it is in favor of improving the preparation process of catalytic membranes and enhancing their stability.

Declaration of competing interest

Rizhi Chen is an editorial board member of Advanced Membranes and was not involved in the editorial review or the decision to publish this article. The authors declare that they have no known competing financial interests or personal relationships that could have appeared to influence the work reported in this paper.

Acknowledgments

The authors are grateful for the financial support from the National Key R&D Program (2022YFB3805504), the National Natural Science Foundation (22208149, 22278209, 22178165, 21921006), and the Natural Science Foundation of Jiangsu Province (BK20220354, BK20211262) of China.

References

[1] S. Miachon, J. Dalmon, Catalysis in membrane reactors: what about the catalyst? Top. Catal. 29 (2004) 59–65.
[2] R. Dittmeyer, K. Svajda, M. Reif, A review of catalytic membrane layers for gas/liquid reactions, Top. Catal. 29 (2004) 3–27.
[3] H.Z. Li, C.L. Qiu, S.J. Ren, Q.B. Dong, S.X. Zhang, F.L. Zhou, X.H. Liang, J.G. Wang, S.G. Li, M. Yu, Na^+-gated water-conducting nanochannels for boosting CO_2 conversion to liquid fuels, Science 367 (2020) 667–671.
[4] U. Aslam, V.G. Rao, S. Chavez, S. Linic, Catalytic conversion of solar to chemical energy on plasmonic metal nanostructures, Nat. Catal. 1 (2018) 656–665.
[5] H. Jiang, Y.F. Liu, W.H. Xing, R.Z. Chen, Porous membrane reactors for liquid-phase heterogeneous catalysis, Ind. Eng. Chem. Res. 60 (2021) 8969–8990.
[6] N.A. Al-Mufachi, N.V. Rees, R. Steinberger-Wilkens, Hydrogen selective membranes: a review of palladium-based dense metal membranes, Renew. Sustain. Energy Rev. 47 (2015) 540–551.
[7] E.E. McLeary, J.C. Jansen, F. Kapteijn, Zeolite based films, membranes and membrane reactors: progress and prospects, Microporous Mesoporous Mater. 90 (2006) 198–220.
[8] V.M. Gryaznov, Mechanism of the catalytic redistribution of hydrogen in unsaturated cyclic hydrocarbons, Russ. Chem. Rev. 4 (1963) 188–200.
[9] H.P. Hsieh, Inorganic membrane reactors - a review, AIChE Sym. Ser. 85 (1989) 53–67.
[10] G. Saracco, V. Specchia, Catalytic inorganic-membrane reactors: present experience and future opportunities, Catal. Rev. 36 (1994) 305–384.
[11] M. Pishnamazi, M. Ghadiri, S. Shirazian, Mathematical modelling and simulation of nitrite hydrogenation in a membrane microreactor, Int. J. Hydrogen Energy 45 (2020) 21555–21566.
[12] R.Z. Chen, Y.G. Jiang, W.H. Xing, W.Q. Jin, Preparation of palladium nanoparticles deposited on a silanized hollow fiber ceramic membrane support and their catalytic properties, Ind. Eng. Chem. Res. 52 (2013) 5002–5008.
[13] X.R. Zhu, Z.W. Pan, H. Jiang, Y. Du, R.Z. Chen, Hierarchical Pd/UiO-66-NH_2-SiO_2 nanofibrous catalytic membrane for highly efficient removal of *p*-nitrophenol, Sep. Purif. Technol. 279 (2021) 119731.
[14] T. Westermann, T. Melin, Flow-through catalytic membrane reactors—principles and applications, Chem. Eng. Process: Process Intensif. 48 (2009) 17–28.
[15] H.Q. Jiang, H.H. Wang, S. Werth, T. Schiestel, J. Caro, Simultaneous production of hydrogen and synthesis gas by combining water splitting with partial oxidation of methane in a hollow-fiber membrane reactor, Angew. Chem., Int. Ed. 47 (2008) 9341–9344.
[16] W.Z. Yue, Y.H. Li, W. Wei, J.W. Jiang, J. Caro, A.S. Huang, Highly selective CO_2 conversion to methanol in a bifunctional zeolite catalytic membrane reactor, Angew. Chem., Int. Ed. 60 (2021) 18289–18294.
[17] L.L. Cai, X. Wu, X.F. Zhu, A.F. Ghoniem, W.S. Yang, High-performance oxygen transport membrane reactors integrated with IGCC for carbon capture, AIChE J. 66 (2020) e16427.
[18] J.F. Miao, J. Lu, H. Jiang, Y.F. Liu, W.H. Xing, X.B. Ke, R.Z. Chen, Continuous and complete conversion of high concentration p-nitrophenol in a flow-through membrane reactor, AIChE J. 65 (2019) e16692.
[19] S.J. Davis, N.S. Lewis, M. Shaner, S. Aggarwal, D. Arent, I.L. Azevedo, S.M. Benson, T. Bradley, J. Brouwer, Y. Chiang, C.T.M. Clack, A. Cohen, S. Doig, J. Edmonds, P. Fennell, C.B. Field, B. Hannegan, B. Hodge, M.I. Hoffert, E. Ingersoll, P. Jaramillo, K.S. Lackner, K.J. Mach, M. Mastrandrea, J. Ogden, P.F. Peterson, D.L. Sanchez, D. Sperling, J. Stagner, J.E. Trancik, C. Yang, K. Caldeira, Net-zero emissions energy systems, Science 360 (2018) eaas9793.
[20] P. Markewitz, W. Kuckshinrichs, W. Leitner, J. Linssen, P. Zapp, R. Bongartz, A. Schreiber, T.E. Müller, Worldwide innovations in the development of carbon capture technologies and the utilization of CO_2, Energy Environ. Sci. 5 (2012) 7281–7305.
[21] J. Franz, V. Scherer, An evaluation of CO_2 and H_2 selective polymeric membranes for CO_2 separation in IGCC processes, J. Membr. Sci. 359 (2010) 173–183.
[22] D.Y.C. Leung, G. Caramanna, M.M. Maroto-Valer, An overview of current status of carbon dioxide capture and storage technologies, Renew. Sustain. Energy Rev. 39 (2014) 426–443.
[23] M. Wang, A. Lawal, P. Stephenson, J. Sidders, C. Ramshaw, Post-combustion CO_2 capture with chemical absorption: a state-of-the-art review, Chem. Eng. Res. Des. 89 (2011) 1609–1624.
[24] P. Luis, T. Van Gerven, B. Van der Bruggen, Recent developments in membrane-based technologies for CO_2 capture, Prog. Energy Combust. Sci. 38 (2012) 419–448.
[25] V. Chou, J. Haslback, N. Kuehn, L.L. Pinkerton, E. Varghese, M.C. Woods, Cost and Performance Baseline for Fossil Energy Plants - Volume 3a: Low Rank Coal to Electricity: IGCC Cases, 2011.
[26] L.Q. Duan, S.Y. Sun, L. Yue, W.J. Qu, Y.P. Yang, Study on a new IGCC (integrated gasification combined cycle) system with CO_2 capture by integrating MCFC (molten carbonate fuel cell), Energy 87 (2015) 490–503.
[27] J. Tonziello, M. Vellini, Oxygen production technologies for IGCC power plants with CO_2 capture, Energy Proc. 4 (2011) 637–644.
[28] R. Anantharaman, O. Bolland, Integration of oxygen transport membranes in an IGCC power plant with CO_2 capture, Chem. Eng. Trans. 25 (2011) 25–30.
[29] G.A. Mutch, L. Qu, G. Triantafyllou, W. Xing, M.-L. Fontaine, I.S. Metcalfe, Supported molten-salt membranes for carbon dioxide permeation, J. Mater. Chem. A 7 (2019) 12951.
[30] P. Zhang, J.J. Tong, K. Huang, X.F. Zhu, W.S. Yang, The current status of high temperature electrochemistry-based CO_2 transport membranes and reactors for direct CO_2 capture and conversion, Prog. Energy Combust. Sci. 82 (2021) 100888.
[31] J.W. Dijkstra, J.A.Z. Pieterse, H. Li, J. Boon, Y.C. van Delft, G. Raju, G. Peppink, R.W. van den Brink, D. Jansen, Development of membrane reactor technology for power production with pre-combustion CO_2 capture, Energy Proc. 4 (2011) 715–722.
[32] A. Giuliano, M. Poletto, D. Barletta, Pure hydrogen co-production by membrane technology in an IGCC power plant with carbon capture, Int. J. Hydrogen Energy 43 (2018) 19279–19292.
[33] P. Chiesa, T.G. Kreutz, G.G. Lozza, CO_2 sequestration from IGCC power plants by means of metallic membranes, J. Eng. Gas Turbines Power 129 (2005) 123–134.
[34] S. Schiebahn, Effizienzoptimierte CO_2-abtrennung in IGCC-Kraftwerken Mittels Wassergas-Shift-Membranreaktoren, Dissertation, Aachen, 2013.
[35] S. Schiebahn, E. Riensche, M. Weber, D. Stolten, Integration of H_2-selective membrane reactors in the integrated gasification combined cycle for CO_2 separation, Chem. Eng. Technol. 35 (2012) 555–560.
[36] H.Y. Gao, Y.S. Lin, Y.D. Li, B.Q. Zhang, Chemical stability and its improvement of palladium-based metallic membranes, Ind. Eng. Chem. Res. 43 (2004) 6920–6930.
[37] M. Gazzani, D.M. Turi, A.F. Ghoniem, E. Macchi, G. Manzolini, Techno-economic assessment of two novel feeding systems for a dry-feed gasifier in an IGCC plant with Pd-membranes for CO_2 capture, Int. J. Greenh. Gas Control 25 (2014) 62–78.
[38] X. Wu, L.L. Cai, X.F. Zhu, A.F. Ghoniem, W.S. Yang, A high-efficiency novel IGCC-OTM carbon capture power plant design, J. Adv. Manuf. Process. 2 (2020) e10059.
[39] A. Evdou, L. Nalbandian, V.T. Zaspalis, Perovskite membrane reactor for continuous and isothermal redox hydrogen production from the dissociation of water, J. Membr. Sci. 325 (2008) 704–711.
[40] C.Y. Park, T.H. Lee, S.E. Dorris, U. Balachandran, Hydrogen production from fossil and renewable sources using an oxygen transport membrane, Int. J. Hydrogen Energy 35 (2010) 4103–4110.
[41] C.Y. Park, T.H. Lee, S.E. Dorris, U. Balachandran, A cobalt-free oxygen transport membrane, $BaFe_{0.9}Zr_{0.1}O_{3-\delta}$, and its application for producing hydrogen, Int. J. Hydrogen Energy 38 (2013) 6450–6459.

[42] W.P. Li, Z.W. Cao, X.F. Zhu, W.S. Yang, High-rate hydrogen separation using an MIEC oxygen permeable membrane reactor, AIChE J. 63 (2017) 1278–1286.
[43] W.P. Li, Z.W. Cao, L.L. Cai, L.X. Zhang, X.F. Zhu, W.S. Yang, H_2S-tolerant oxygen-permeable ceramic membranes for hydrogen separation with a performance comparable to those of palladium-based membranes, Energy Environ. Sci. 10 (2017) 101–106.
[44] X.F. Zhu, Q.M. Li, Y. Cong, W.S. Yang, Syngas generation in a membrane reactor with a highly stable ceramic composite membrane, Catal. Commun. 10 (2008) 309–312.
[45] L.L. Cai, S.Q. Hu, Z.W. Cao, H.B. Li, X.F. Zhu, W.S. Yang, Dual-phase membrane reactor for hydrogen separation with high tolerance to CO_2 and H_2S impurities, AIChE J. 65 (2019) 1088–1096.
[46] L.L. Cai, W.P. Li, Z.W. Cao, X.F. Zhu, W.S. Yang, Improving oxygen permeation of MIEC membrane reactor by enhancing the electronic conductivity under intermediate-low oxygen partial pressures, J. Membr. Sci. 520 (2016) 607–615.
[47] X. Wu, A.F. Ghoniem, M. Uddi, Enhancing co-production of H_2 and syngas via water splitting and POM on surface-modified oxygen permeable membranes, AIChE J. 62 (2016) 4427–4435.
[48] L.J. Jia, G.H. He, Y. Zhang, J. Caro, H.Q. Jiang, Hydrogen purification through a highly stable dual-phase oxygen-permeable membrane, Angew. Chem., Int. Ed. 60 (2021) 5204–5208.
[49] W.P. Li, Z.W. Cao, X.F. Zhu, W.S. Yang, Effects of membrane thickness and structural type on the hydrogen separation performance of oxygen-permeable membrane reactors, J. Membr. Sci. 573 (2019) 370–376.
[50] L.L. Cai, Y. Zhu, Z.W. Cao, W.P. Li, H.B. Li, X.F. Zhu, W.S. Yang, Non-noble metal catalysts coated on oxygen-permeable membrane reactors for hydrogen separation, J. Membr. Sci. 594 (2020) 117463.
[51] L.L. Cai, Z.W. Cao, X.F. Zhu, W.S. Yang, Improved hydrogen separation performance of asymmetric oxygen transport membranes by grooving in the porous support layer, Green Chem. Eng. 2 (2021) 96–103.
[52] J.L. Hong, , H.B. GDC-GSTA Wang, S. Gopalan, U. Pal, Effect of surface-exchange catalyst on the transport properties of MIEC membrane for hydrogen separation, ECS Trans. 6 (2008) 1.
[53] L.L. Cai, W. Liu, Z.W. Cao, H.B. Li, Y. Cong, X.F. Zhu, W.S. Yang, Effect of Ru and Ni nanocatalysts on water splitting and hydrogen oxidation reactions in oxygen-permeable membrane reactors, J. Membr. Sci. 599 (2020) 117702.
[54] L.L. Cai, Z.W. Cao, X.F. Zhu, W.S. Yang, Effects of catalysts on water decomposition and hydrogen oxidation reactions in oxygen transport membrane reactors, J. Membr. Sci. 634 (2021) 119394.
[55] L.L. Cai, J.Y. Wang, X.F. Zhu, Recent progress on mixed conducting oxygen transport membrane reactors for water splitting reaction, Hua Hsueh Hsueh Pao 79 (2021) 588.
[56] X.F. Zhu, W.S. Yang, Microstructural and interfacial designs of oxygen-permeable membranes for oxygen separation and reaction-separation coupling, Adv. Mater. 31 (2019) 1902547.
[57] J.L. Chi, K.Y. Li, S.J. Zhang, X.F. Zhu, L.F. Zhao, B. Wang, Y.H. Xiao, Process simulation and integration of IGCC systems with novel mixed ionic and electronic conducting membrane-based water gas shift membrane reactors for CO_2 capture, Int. J. Hydrogen Energy 45 (2020) 13884–13898.
[58] P. Cox, C. Jones, Illuminating the modern dance of climate and CO_2, Science 321 (2008) 1642–1644.
[59] W. Wang, S.P. Wang, X.B. Ma, J.L. Gong, Recent advances in catalytic hydrogenation of carbon dioxide, Chem. Soc. Rev. 40 (2011) 3703–3727.
[60] A. Álvarez, A. Bansode, A. Urakawa, A.V. Bavykina, T.A. Wezendonk, M. Makkee, J. Gascon, F. Kapteijn, Challenges in the greener production of formates/formic acid, methanol, and DME by heterogeneously catalyzed CO_2 hydrogenation processes, Chem. Rev. 117 (2017) 9804–9838.
[61] J.W. Zhong, X.F. Yang, Z.L. Wu, B.L. Liang, Y.Q. Huang, T. Zhang, State of the art and perspectives in heterogeneous catalysis of CO_2 hydrogenation to methanol, Chem. Soc. Rev. 49 (2020) 1385–1413.
[62] C. Arcoumanis, C. Bae, R. Crookes, E. Kinoshita, The potential of di-methyl ether (DME) as an alternative fuel for compression-ignition engines: a review, Fuel 87 (2008) 1014–1030.
[63] E.C. Ra, K.Y. Kim, E.H. Kim, H. Lee, K. An, J.S. Lee, Recycling carbon dioxide through catalytic hydrogenation: recent key developments and perspectives, ACS Catal. 10 (2020) 11318–11345.
[64] D. Xu, Y.Q. Wang, M.Y. Ding, X.L. Hong, G.L. Liu, S.C.E. Tsang, Advances in higher alcohol synthesis from CO_2 hydrogenation, Chem 7 (2021) 849–881.
[65] C. Baltes, S. Vukojević, F. Schüth, Correlations between synthesis, precursor, and catalyst structure and activity of a large set of $CuO/ZnO/Al_2O_3$ catalysts for methanol synthesis, J. Catal. 258 (2008) 334–344.
[66] K.H. Sun, Z.G. Fan, J.Y. Ye, J.M. Yan, Q.F. Ge, Y.N. Li, W.J. He, W.M. Yang, C. Liu, Hydrogenation of CO_2 to methanol over In_2O_3 catalyst, J. CO_2 Util. 12 (2015) 1–6.
[67] X. Jiang, N. Koizumi, X.W. Guo, C.S. Song, Bimetallic Pd-Cu catalysts for selective CO_2 hydrogenation to methanol, Appl. Catal. B Environ. 170–171 (2015) 173–185.
[68] K. Chang, T.F. Wang, J.G. Chen, Hydrogenation of CO_2 to methanol over $CuCeTiO_x$ catalysts, Appl. Catal. B Environ. 206 (2017) 704–711.
[69] J.J. Wang, G.N. Li, Z.L. Li, C.Z. Tang, Z.C. Feng, H.Y. An, H.L. Liu, T.F. Liu, C. Li, A highly selective and stable $ZnO\text{-}ZrO_2$ solid solution catalyst for CO_2 hydrogenation to methanol, Sci. Adv. 3 (2017) e1701290.
[70] Y.H. Wang, S. Kattel, W.G. Gao, K.Z. Li, P. Liu, J.G. Chen, H. Wang, Exploring the ternary interactions in $Cu\text{-}ZnO\text{-}ZrO_2$ catalysts for efficient CO_2 hydrogenation to methanol, Nat. Commun. 10 (2019) 1166.
[71] C.S. Yang, C.L. Pei, R. Luo, S.H. Liu, Y.N. Wang, Z.Y. Wang, Z.J. Zhao, J.L. Gong, Strong electronic oxide-support interaction over In_2O_3/ZrO_2 for highly selective CO_2 hydrogenation to methanol, J. Am. Chem. Soc. 142 (2020) 19523–19531.
[72] S.S. Dang, B. Qin, Y. Yang, H. Wang, J. Cai, Y. Han, S.G. Li, P. Gao, Y.H. Sun, Rationally designed indium oxide catalysts for CO_2 hydrogenation to methanol with high activity and selectivity, Sci. Adv. 6 (2020) eaaz2060.
[73] C. Meng, G.F. Zhao, X.R. Shi, P.J. Chen, Y. Liu, Y. Lu, Oxygen-deficient metal oxides supported nano-intermetallic $InNi_3C_{0.5}$ toward efficient CO_2 hydrogenation to methanol, Sci. Adv. 7 (2021) eabi6012.
[74] A. Liu, M.F. Gao, X.F. Ren, F.N. Meng, Y.N. Yang, L.G. Gao, Q.Y. Yang, T.L. Ma, Current progress in electrocatalytic carbon dioxide reduction to fuels on heterogeneous catalysts, J. Mater. Chem. A 8 (2020) 3541–3562.
[75] D. Gao, R.M. Aran-Ais, H.S. Jeon, B.R. Cuenya, Rational catalyst and electrolyte design for CO_2 electroreduction towards multicarbon products, Nat. Catal. 2 (2019) 198–210.
[76] S. Xu, E.A. Carter, Theoretical insights into heterogeneous (photo)electrochemical CO_2 reduction, Chem. Rev. 119 (11) (2019) 6631–6669.
[77] J. Wu, T. Sharifi, Y. Gao, T. Zhang, P.M. Ajayan, Emerging carbon-based heterogeneous catalysts for electrochemical reduction of carbon dioxide into value-added chemicals, Adv. Mater. 31 (2019) 1804257.
[78] K. Zhao, X. Quan, Carbon-based materials for electrochemical reduction of CO_2 to C2+ oxygenates: recent progress and remaining challenges, ACS Catal. 11 (2021) 2076–2097.
[79] I. Ro, Y.F. Liu, M.R. Ball, D.H.K. Jackson, J.P. Chada, C. Sener, T.F. Kuech, R.J. Madon, G.W. Huber, J.A. Dumesic, Role of the $Cu\text{-}ZrO_2$ interfacial sites for conversion of ethanol to ethyl acetate and synthesis of methanol from CO_2 and H_2, ACS Catal. 6 (2016) 7040–7050.
[80] I.A. Fisher, A.T. Bell, In-situ infrared study of methanol synthesis from H_2/CO_2 over Cu/SiO_2 and $Cu/ZrO_2/SiO_2$, J. Catal. 172 (1997) 222–237.
[81] E. Frei, A. Schaadt, T. Ludwig, H. Hillebrecht, I. Krossing, The influence of the precipitation/ageing temperature on a $Cu/ZnO/ZrO_2$ catalyst for methanol synthesis from H_2 and CO_2, ChemCatChem 6 (2014) 1721–1730.
[82] S. Natesakhawat, J.W. Lekse, J.P. Baltrus, P.R. Ohodnicki Jr., B.H. Howard, X. Deng, C. Matranga, Active sites and structure-activity relationships of copper-based catalysts for carbon dioxide hydrogenation to methanol, ACS Catal. 2 (2012) 1667–1676.
[83] R. Ladera, F.J. Pérez-Alonso, J.M. González-Carballo, M. Ojeda, S. Rojas, J.L.G. Fierro, Catalytic valorization of CO_2 via methanol synthesis with Ga-promoted $Cu\text{-}ZnO\text{-}ZrO_2$ catalysts, Appl. Catal. B Environ. 142–143 (2013) 241–248.
[84] C.T. Campbell, C.H.F. Peden, Oxygen vacancies and catalysis on ceria surfaces, Science 309 (2005) 713–714.
[85] F. Arena, G. Mezzatesta, G. Zafarana, G. Trunfio, F. Frusteri, L. Spadaro, How oxide carriers control the catalytic functionality of the Cu-ZnO system in the hydrogenation of CO_2 to methanol, Catal. Today 210 (2013) 39–46.
[86] F. Arena, G. Italiano, K. Barbera, G. Bonura, L. Spadaro, F. Frusteri, Basic evidences for methanol-synthesis catalyst design, Catal. Today 143 (2009) 80–85.
[87] L. Li, D.S. Mao, J. Yu, X.M. Guo, Highly selective hydrogenation of CO_2 to methanol over $CuO\text{-}ZnO\text{-}ZrO_2$ catalysts prepared by a surfactant-assisted co-precipitation method, J. Power Sources 279 (2015) 394–404.
[88] T.Q.J. Qi, Y.M. Zhao, S.Y. Chen, W.Z. Li, X.W. Guo, Y.C. Zhang, C.S. Song, Bimetallic metal organic framework-templated synthesis of a $Cu\text{-}ZnO/Al_2O_3$ catalyst with superior methanol selectivity for CO_2 hydrogenation, Mol. Catal. 514 (2021) 111870.
[89] H. Bahruji, M. Bowker, G. Hutchings, N. Dimitratos, P. Wells, E. Gibson, W. Jones, C. Brookes, D. Morgan, G. Lalev, Pd/ZnO catalysts for direct CO_2 hydrogenation to methanol, J. Catal. 343 (2016) 133–146.
[90] Y.Z. Yin, B. Hu, X.L. Li, X.H. Zhou, X.L. Hong, G.L. Liu, Pd@zeolitic imidazolate framework-8 derived PdZn alloy catalysts for efficient hydrogenation of CO_2 to methanol, Appl. Catal. B Environ. 234 (2018) 143–152.
[91] X.L. Li, Z.Y. Zeng, B. Hu, L.H. Qian, X.L. Hong, Surface-atom dependence of ZnO-supported Ag@Pd core@shell nanocatalysts in CO_2 hydrogenation to CH_3OH, ChemCatChem 9 (2017) 924–928.
[92] T.K. Liu, D. Xu, D.D. Wu, G.L. Liu, X.L. Hong, Spinel $ZnFe_2O_4$ regulates copper sites for CO_2 hydrogenation to methanol, ACS Sustain. Chem. Eng. 9 (2021) 4033–4041.
[93] B.L. Liang, J.G. Ma, X. Su, C.Y. Yang, H.M. Duan, H.W. Zhou, S.L. Deng, L. Li, Y.Q. Huang, Investigation on deactivation of $Cu/ZnO/Al_2O_3$ catalyst for CO_2 hydrogenation to methanol, Ind. Eng. Chem. Res. 58 (2019) 9030–9037.
[94] A. Prašnikar, A. Pavlišič, F. Ruiz-Zepeda, J. Kovač, B. Likozar, Mechanisms of copper-based catalyst deactivation during CO2 reduction to methanol, Ind. Eng. Chem. Res. 58 (2019) 13021–13029.
[95] R.P.W.J. Struis, M. Quintilii, S. Stucki, Feasibility of Li-Nafion hollow fiber membranes in methanol synthesis: mechanical and thermal stability at elevated temperature and pressure, J. Membr. Sci. 177 (2000) 215–223.
[96] U. Illgen, R. Schäfer, M. Noack, P. Kölsch, A. Kühnle, J. Caro, Membrane supported catalytic dehydrogenation of iso-butane using an MFI zeolite membrane reactor, Catal. Commun. 2 (2001) 339–345.
[97] B. Jeong, K. Sotowa, K. Kusakabe, Catalytic dehydrogenation of cyclohexane in an FAU-type zeolite membrane reactor, J. Membr. Sci. 224 (2003) 151–158.
[98] T. Masuda, T. Asanuma, M. Shouji, S.R. Mukai, M. Kawase, K. Hashimoto, Methanol to olefins using ZSM-5 zeolite catalyst membrane reactor, Chem. Eng. Sci. 58 (2003) 649–656.
[99] C. Zhang, Z. Hong, X.H. Gu, Z.X. Zhong, W.Q. Jin, N.P. Xu, Silicalite-1 zeolite membrane reactor packed with HZSM-5 catalyst for meta-xylene isomerization, Ind. Eng. Chem. Res. 48 (2009) 4293–4299.

[100] C.L. Kong, J.M. Lu, J.H. Yang, J.Q. Wang, Catalytic dehydrogenation of ethylbenzene to styrene in a zeolite silicalite-1 membrane reactor, J. Membr. Sci. 306 (2007) 29–35.

[101] Z. Tang, S. Kim, G.K. Reddy, J.H. Dong, P. Smirniotis, Modified zeolite membrane reactor for high temperature water gas shift reaction, J. Membr. Sci. 354 (2010) 114–122.

[102] S. Khajavi, J.C. Jansen, F. Kapteijn, Application of a sodalite membrane reactor in esterification-Coupling reaction and separation, Catal. Today 156 (2010) 132–139.

[103] C. Zhou, N.Y. Wang, Y.N. Qian, X.X. Liu, J. Caro, A.S. Huang, Efficient synthesis of dimethyl ether from methanol in a bifunctional zeolite membrane reactor, Angew. Chem., Int. Ed. 55 (2016) 12678–12682.

[104] W.Z. Yue, Z. Wan, Y.H. Li, X. He, J. Caro, A.S. Huang, Synthesis of Cu-ZnO-Pt@HZSM-5 catalytic membrane reactor for CO_2 hydrogenation to dimethyl ether, J. Membr. Sci. 660 (2022) 120845.

[105] A.S. Huang, W.S. Yang, J. Liu, Synthesis and pervaporation properties of NaA zeolite membranes prepared with vacuum-assisted method, Sep. Purif. Technol. 56 (2007) 158–167.

[106] K. Sato, K. Aoki, K. Sugimoto, K. Izumi, S. Inoue, J. Saito, S. Ikeda, T. Nakane, Dehydrating performance of commercial LTA zeolite membranes and application to fuel grade bio-ethanol production by hybrid distillation/vapor permeation process, Microporous Mesoporous Mater. 115 (2008) 184–188.

[107] J. Caro, D. Albrecht, M. Noack, Why is it so extremely difficult to prepare shape-selective Al-rich zeolite membranes like LTA and FAU for gas separation? Sep. Purif. Technol. 66 (2009) 143–147.

[108] A.S. Huang, Y.S. Lin, W.S. Yang, Synthesis and properties of A-type zeolite membranes by secondary growth method with vacuum seeding, J. Membr. Sci. 245 (2004) 41–51.

[109] X.C. Xu, W.S. Yang, J. Liu, L.W. Lin, Synthesis of NaA zeolite membranes from clear solution, Microporous Mesoporous Mater. 43 (2001) 299–311.

[110] X. Xu, W. Yang, J. Liu, L. Lin, Synthesis of a high-permeance NaA zeolite membrane by microwave heating, Adv. Mater. 12 (2000) 195–198.

[111] F. Tiscareño-Lechuga, C. Téllez, M. Menéndez, X. Santamarı, J. A, A novel device for preparing zeolite—a membranes under a centrifugal force field, J. Membr. Sci. 212 (2003) 135–146.

[112] A.S. Huang, W.S. Yang, Hydrothermal synthesis of uniform and dense NaA zeolite membrane in the electric field, Microporous Mesoporous Mater. 102 (2007) 58–69.

[113] A.S. Huang, F.Y. Liang, F. Steinbach, J. Caro, Preparation and separation properties of LTA membranes by using 3-aminopropyltriethoxysilane as covalent linker, J. Membr. Sci. 350 (2010) 5–9.

[114] A.S. Huang, N.Y. Wang, J. Caro, Seeding-free synthesis of dense zeolite FAU membranes on 3-aminopropyltriethoxysilane-functionalized alumina supports, J. Membr. Sci. 389 (2012) 272–279.

[115] A.S. Huang, J. Caro, Facile synthesis of LTA molecular sieve membranes on covalently functionalized supports by using diisocyanates as molecular linkers, J. Mater. Chem. 21 (2011) 11424–11429.

[116] C.F. Yuan, Q. Liu, H.F. Chen, A.S. Huang, Mussel-inspired polydopamine modification of supports for the facile synthesis of zeolite LTA molecular sieve membranes, RSC Adv. 4 (2014) 41982–41988.

[117] F. Dawood, M. Anda, G.M. Shafiullah, Hydrogen production for energy: an overview, Int. J. Hydrogen Energy 45 (2020) 3847–3869.

[118] S. Adhikari, S. Fernando, Hydrogen membrane separation techniques, Ind. Eng. Chem. Res. 45 (2006) 875–881.

[119] S. Sircar, T.C. Golden, Purification of hydrogen by pressure swing adsorption, Separ. Sci. Technol. 35 (2000) 667–687.

[120] G.J. Grashoff, C.E. Pilkington, C.W. Corti, Purification of hydrogen, platin, Met. Rev. 27 (1983) 157–169.

[121] S. Yan, H. Maeda, K. Kusakabe, S. Morooka, Thin palladium membrane formed in support pores by metal-organic chemical vapor deposition method and application to hydrogen separation, Ind. Eng. Chem. Res. 33 (1994) 616–622.

[122] M.R. Rahimpour, F. Samimi, A. Babapoor, T. Tohidian, S. Mohebi, Palladium membranes applications in reaction systems for hydrogen separation and purification: a review, Chem. Eng. Process: Process Intensif. 121 (2017) 24–49.

[123] E. Drioli, G. Barbieri, A. Brunetti, E. Drioli, G. Barbieri, A. Brunetti, Membrane Engineering for the Treatment of Gases: Volume 2: Gas-separation Issues Combined with Membrane Reactors, The Royal Society of Chemistry, 2017.

[124] L. Roses, G. Manzolini, S. Campanari, E. De Wit, M. Walter, Techno-economic assessment of membrane reactor technologies for pure hydrogen production for fuel cell vehicle fleets, Energy Fuels 27 (2013) 4423–4431.

[125] M. Abdollahi, J. Yu, P.K.T. Liu, R. Ciora, M. Sahimi, T.T. Tsotsis, Ultra-pure hydrogen production from reformate mixtures using a palladium membrane reactor system, J. Membr. Sci. 390–391 (2012) 32–42.

[126] Y. Lin, M. Rei, Process development for generating high purity hydrogen by using supported palladium membrane reactor as steam reformer, Int. J. Hydrogen Energy 25 (2000) 211–219.

[127] Y. Shirasaki, T. Tsuneki, Y. Ota, I. Yasuda, S. Tachibana, H. Nakajima, K. Kobayashi, Development of membrane reformer system for highly efficient hydrogen production from natural gas, Int. J. Hydrogen Energy 34 (2009) 4482–4487.

[128] E. Fernandez, J.A. Medrano, J. Melendez, M. Parco, J.L. Viviente, M. van Sint Annaland, F. Gallucci, D.A. Pacheco Tanaka, Preparation and characterization of metallic supported thin Pd-Ag membranes for hydrogen separation, Chem. Eng. J. 305 (2016) 182–190.

[129] C.G. Sonwane, J. Wilcox, Y.H. Ma, Solubility of hydrogen in PdAg and PdAu binary alloys using density functional theory, J. Phys. Chem. B 110 (2006) 24549–24558.

[130] H.Y. Jia, P. Wu, G.F. Zeng, E. Salas-Colera, A. Serrano, G.R. Castro, H.Y. Xu, C.L. Sun, A. Goldbach, High-temperature stability of Pd alloy membranes containing Cu and Au, J. Membr. Sci. 544 (2017) 151–160.

[131] C.Y. Zhao, A. Goldbach, H.Y. Xu, Low-temperature stability of body-centered cubic PdCu membranes, J. Membr. Sci. 542 (2017) 60–67.

[132] N. Chandrasekhar, D.S. Sholl, Computational study of hydrogen induced lattice rearrangement and its influence on hydrogen permeance in Pd-Au alloys, J. Alloys Compd. 609 (2014) 244–252.

[133] J.X. Liu, S. Bellini, N.C.A. de Nooijer, Y. Sun, D.A. Pacheco Tanaka, C.H. Tang, H. Li, F. Gallucci, A. Caravella, Hydrogen permeation and stability in ultra-thin PdRu supported membranes, Int. J. Hydrogen Energy 45 (2020) 7455–7467.

[134] H.W. Abu El Hawa, S.N. Paglieri, C.C. Morris, A. Harale, J. Douglas Way, Application of a Pd–Ru composite membrane to hydrogen production in a high temperature membrane reactor, Sep. Purif. Technol. 147 (2015) 388–397.

[135] T. Wang, Z. Fan, S. Wang, Q. Zheng, J. Tan, Z. Liu, G. Zhang, W. Jin, One-step thermal processing of BaCe0.8Y0.2O3-δ hydrogen permeable multichannel hollow fiber membrane, AIChE J. 68 (2022) e17603.

[136] M. Yang, F. He, C. Zhou, F. Dong, G. Yang, W. Zhou, Z. Shao, New perovskite membrane with improved sintering and self-reconstructed surface for efficient hydrogen permeation, J. Membr. Sci. 620 (2021) 118980.

[137] H. Iwahara, T. Esaka, H. Uchida, N. Maeda, Proton conduction in sintered oxides and its application to steam electrolysis for hydrogen production, Solid State Ionics 3–4 (1981) 359–363.

[138] X.W. Qi, Y.S. Lin, Electrical conduction and hydrogen permeation through mixed proton-electron conducting strontium cerate membranes, Solid State Ionics 130 (2000) 149–156.

[139] X.T. Wei, J. Kniep, Y.S. Lin, Hydrogen permeation through terbium doped strontium cerate membranes enabled by presence of reducing gas in the downstream, J. Membr. Sci. 345 (2009) 201–206.

[140] H.M. Zhang, B.A. Wilhite, Electrical conduction and hydrogen permeation investigation on iron-doped barium zirconate membrane, J. Membr. Sci. 512 (2016) 104–110.

[141] W.H. Yuan, C.C. Xiao, L. Li, Hydrogen permeation and chemical stability of In-doped $SrCe_{0.95}Tm_{0.05}O_3$-δ membranes, J. Alloys Compd. 616 (2014) 142–147.

[142] X.H. Tan, X.Y. Tan, N.T. Yang, B. Meng, K. Zhang, S.M. Liu, High performance $BaCe_{0.8}Y_{0.2}O_3$-a (BCY) hollow fibre membranes for hydrogen permeation, Ceram. Int. 40 (2014) 3131–3138.

[143] S. Escolástico, M. Ivanova, C. Solís, S. Roitsch, W.A. Meulenberg, J.M. Serra, Improvement of transport properties and hydrogen permeation of chemically-stable proton-conducting oxides based on the system $BaZr_{1-x-y}Y_xMyO_3$-δ, RSC Adv. 2 (2012) 4932–4943.

[144] G. Chiodelli, L. Malavasi, C. Tealdi, S. Barison, M. Battagliarin, L. Doubova, M. Fabrizio, C. Mortalò, R. Gerbasi, Role of synthetic route on the transport properties of $BaCe_{1-x}Y_xO_3$ proton conductor, J. Alloys Compd. 470 (2009) 477–485.

[145] G.W. Weng, K. Ouyang, X.H. Lin, S.I. Wen, Y.S. Zhou, S. Lei, J. Xue, H.H. Wang, Enhanced hydrogen permeability of mixed protonic-electronic conducting membranes through an in-situ exsolution strategy, Adv. Funct. Mater. 32 (2022) 2205255.

[146] Y.Y. Wei, J. Xue, W. Fang, Y. Chen, H.H. Wang, J. Caro, Enhanced stability of Zr-doped Ba(CeTb)O_3-δ-Ni cermet membrane for hydrogen separation, Chem. Commun. 51 (2015) 11619–11621.

[147] H. Kim, B. Kim, J. Lee, K. Ahn, H. Kim, K.J. Yoon, B. Kim, Y.W. Cho, H. Lee, J. Lee, Microstructural adjustment of Ni-$BaCe_{0.9}Y_{0.1}O_3$-δ cermet membrane for improved hydrogen permeation, Ceram. Int. 40 (2014) 4117–4126.

[148] Y.C. Tsai, C.C. Lin, W.L. Lin, J.H. Wang, S.Y. Chen, P. Lin, P.W. Wu, Palladium based cermet composite for hydrogen separation at elevated temperature, J. Power Sources 274 (2015) 965–970.

[149] W.A. Rosensteel, N.P. Sullivan, Fabrication and hydrogen permeation through novel $BaZr_{0.9}Y_{0.1}O_3$-δ-Cu composite ceramic-metallic membranes, Int. J. Hydrogen Energy 42 (2017) 4216–4223.

[150] E. Rebollo, C. Mortalò, S. Escolástico, S. Boldrini, S. Barison, J.M. Serra, M. Fabrizio, Exceptional hydrogen permeation of all-ceramic composite robust membranes based on $BaCe_{0.65}Zr_{0.20}Y_{0.15}O_3$.δ and Y- or Gd-doped ceria, Energy Environ. Sci. 8 (2015) 3675–3686.

[151] S.F. Cheng, Y.J. Wang, L.B. Zhuang, J. Xue, Y.Y. Wei, A. Feldhoff, J. Caro, H.H. Wang, A dual-phase ceramic membrane with extremely high H_2 permeation flux prepared by autoseparation of a ceramic precursor, Angew. Chem., Int. Ed. 55 (2016) 10895–10898.

[152] W.P. Li, X.F. Zhu, Z.W. Cao, W.P. Wang, W.S. Yang, Mixed ionic-electronic conducting (MIEC) membranes for hydrogen production from water splitting, Int. J. Hydrogen Energy 40 (2015) 3452–3461.

[153] S.J. Son, H.J. Lee, S.K. Kim, J.-H. Lee, H.J. Park, J.H. Joo, Exceptional performance of water splitting coupled with methane partial oxidation by oxygen-permeable membrane reactor, Chem. Eng. J. 466 (2023) 143031.

[154] G. He, Q. Lan, M. Liu, G. Wu, R.E. Dunin-Borkowski, H. Jiang, Multilayered ceramic membrane with ion conducting thin layer induced by interface reaction for stable hydrogen production, Angew. Chem. Int. Ed. 62 (2023) e202210485.

[155] H. Naito, H. Arashi, Hydrogen production from direct water splitting at high temperatures using a ZrO_2-TiO_2-Y_2O_3 membrane, Solid State Ionics 79 (1995) 366–370.

[156] N. Zhu, X.L. Dong, Z.K. Liu, G.R. Zhang, W.Q. Jin, N.P. Xu, Toward highly-effective and sustainable hydrogen production: bio-ethanol oxidative steam reforming

coupled with water splitting in a thin tubular membrane reactor, Chem. Commun. 48 (2012) 7137–7139.
[157] H.Q. Jiang, Z.W. Cao, S. Schirrmeister, T. Schiestel, J. Caro, A coupling strategy to produce hydrogen and ethylene in a membrane reactor, Angew. Chem., Int. Ed. 49 (2010) 5656–5660.
[158] H.Q. Jiang, F.Y. Liang, O. Czuprat, K. Efimov, A. Feldhoff, S. Schirrmeister, T. Schiestel, H.H. Wang, J. Caro, Hydrogen production by water dissociation in surface-modified $BaCo_xFeyZr_{1-x-y}O_3.\delta$ hollow-fiber membrane reactor with improved oxygen permeation, Chem. Eur J. 16 (2010) 7898–7903.
[159] A. Wang, M. Liang, Q.Y. Xiang, J. Xue, H.H. Wang, Mixed oxygen ionic and electronic conducting membrane reactors for pure chemicals production, Chem. Ing. Tech. 94 (2022) 31–41.
[160] G.H. He, W.Y. Liang, C. Tsai, X.L. Xia, S. Baumann, H.Q. Jiang, W.A. Meulenberg, Chemical environment-induced mixed conductivity of titanate as a highly stable oxygen transport membrane, iScience 19 (2019) 955–964.
[161] H.B. Wang, S. Gopalan, U.B. Pal, Hydrogen generation and separation using $Gd_{0.2}Ce_{0.8}O_{1.9}$-δ–$Gd_{0.08}Sr_{0.88}Ti_{0.95}Al_{0.05}O_{3\pm}\delta$ mixed ionic and electronic conducting membranes, Electrochim. Acta 56 (2011) 6989–6996.
[162] H.D. Cui, A. Karthikeyan, S. Gopalan, U.B. Pal, $Gd_{0.2}Ce_{0.8}O_{1.9}$-$Y_{0.08}Sr_{0.88}Ti_{0.95}Al_{0.05}O_{3-}\delta$ composite mixed conductors for hydrogen separation, J. Electrochem. Soc. 152 (2005) A1726.
[163] T.V. Choudhary, V.R. Choudhary, Energy-efficient syngas production through catalytic oxy-methane reforming reactions, Angew. Chem., Int. Ed. 47 (2008) 1828–1847.
[164] Q.H. Zhang, J.C. Kang, Y. Wang, Development of novel catalysts for fischer-tropsch synthesis: tuning the product selectivity, ChemCatChem 2 (2010) 1030–1058.
[165] H. Malerød-Fjeld, D. Clark, I. Yuste-Tirados, R. Zanón, D. Catalán-Martinez, D. Beeaff, S.H. Morejudo, P.K. Vestre, T. Norby, R. Haugsrud, J.M. Serra, C. Kjølseth, Thermo-electrochemical production of compressed hydrogen from methane with near-zero energy loss, Nat. Energy 2 (2017) 923–931.
[166] X.L. Xia, H.Y. Zhou, Y. Zhang, H.Q. Jiang, Innovative steam methane reforming for coproducing CO-free hydrogen and syngas in proton conducting membrane reactor, AIChE J. 65 (2019) e16740.
[167] T. Ishihara, Y. Takita, Partial oxidation of methane into syngas with oxygen permeating ceramic membrane reactors, Catal. Surv. Jpn. 4 (2001) 125–133.
[168] C. Tsai, A.G. Dixon, W.R. Moser, Y.H. Ma, Dense perovskite membrane reactors for partial oxidation of methane to syngas, AIChE J. 43 (1997) 2741–2750.
[169] E.V. Kondratenko, H.H. Wang, V.A. Kondratenko, J. Caro, Selective oxidation of CH_4 and C_2H_6 over a mixed oxygen ion and electron conducting perovskite—a TAP and membrane reactors study, J. Mol. Catal. Chem. 297 (2009) 142–149.
[170] X.Y. Tan, L.L. Shi, G.Z. Hao, B. Meng, S.M. Liu, $La_{0.7}Sr_{0.3}FeO_3$.α perovskite hollow fiber membranes for oxygen permeation and methane conversion, Sep. Purif. Technol. 96 (2012) 89–97.
[171] K.P. Jiang, Z.K. Liu, G.R. Zhang, W.Q. Jin, A novel catalytic membrane reactor with homologous exsolution-based perovskite catalyst, J. Membr. Sci. 608 (2020) 118213.
[172] Z.G. Wang, J. Ashok, Z.W. Pu, S. Kawi, Low temperature partial oxidation of methane via $BaBi_{0.05}Co_{0.8}Nb_{0.15}O_3$-δ-Ni phyllosilicate catalytic hollow fiber membrane reactor, Chem. Eng. J. 315 (2017) 315–323.
[173] H.H. Wang, A. Feldhoff, J. Caro, T. Schiestel, S. Werth, Oxygen selective ceramic hollow fiber membranes for partial oxidation of methane, AIChE J. 55 (2009) 2657–2664.
[174] X.F. Zhu, Y. Cong, W.S. Yang, Oxygen permeability and structural stability of $BaCe_{0.15}Fe_{0.85}O_3$-δ membranes, J. Membr. Sci. 283 (2006) 38–44.
[175] W. Chen, Y.B. Zuo, C.S. Chen, A.J.A. Winnubst, Effect of Zr^{4+} doping on the oxygen stoichiometry and phase stability of $SrCo_{0.8}Fe_{0.2}O_3.\delta$ oxygen separation membrane, Solid State Ionics 181 (2010) 971–975.
[176] M.C. Zhan, H. Ren, T.F. Tian, W.D. Wang, C.S. Chen, Effects of hydrogen treatment on the surface microstructure and oxygen permeability of $La_{0.7}Sr_{0.3}Ga_{0.3}Fe_{0.7}O_3.\delta$ membrane, Solid State Ionics 179 (2008) 1382–1386.
[177] V.V. Kharton, A.L. Shaula, F.M.M. Snijkers, J.F.C. Cooymans, J.J. Luyten, A.A. Yaremchenko, A.A. Valente, E.V. Tsipis, J.R. Frade, F.M.B. Marques, J. Rocha, Processing, stability and oxygen permeability of Sr(Fe, Al)O_3-based ceramic membranes, J. Membr. Sci. 252 (2005) 215–225.
[178] H. Wang, C. Tablet, A. Feldhoff, J. Caro, A cobalt-free oxygen-permeable membrane based on the perovskite-type oxide $Ba_{0.5}Sr_{0.5}Zn_{0.2}Fe_{0.8}O_3.\delta$, Adv. Mater. 17 (2005) 1785–1788.
[179] J. Sunarso, S.S. Hashim, N. Zhu, W. Zhou, Perovskite oxides applications in high temperature oxygen separation, solid oxide fuel cell and membrane reactor: a review, Prog. Energy Combust. Sci. 61 (2017) 57–77.
[180] A.S. Ghanem, F. Liang, M. Liu, H. Jiang, A. Toghan, Hydrogen production by water splitting coupled with the oxidation of coke oven gas in a catalytic oxygen transport membrane reactor, Chem. Eng. J. 474 (2023) 145263.
[181] S.H. Morejudo, R. Zanón, S. Escolástico, I. Yuste-Tirados, H. Malerød-Fjeld, P.K. Vestre, W.G. Coors, A. Martínez, T. Norby, J.M. Serra, C. Kjølseth, Direct conversion of methane to aromatics in a catalytic co-ionic membrane reactor, Science 353 (2016) 563–566.
[182] T. Wei, L.C. Jia, J. Luo, B. Chi, J. Pu, J. Li, CO_2 dry reforming of CH_4 with Sr and Ni co-doped $LaCrO_3$ perovskite catalysts, Appl. Surf. Sci. 506 (2020) 144699.
[183] G.H. He, T.M. Hu, H.Y. Zhou, F.Y. Liang, S. Baumann, W.A. Meulenberg, H.Q. Jiang, Syngas production by biogas reforming in a redox-stable and CO_2-tolerant oxygen transporting membrane reactor, Ind. Eng. Chem. Res. 56 (2017) 10134–10141.
[184] W.Y. Liang, Z.W. Cao, G.H. He, J. Caro, H.Q. Jiang, Oxygen transport membrane for thermochemical conversion of water and carbon dioxide into synthesis gas, ACS Sustain. Chem. Eng. 5 (2017) 8657–8662.
[185] X.Y. Gao, S.K. Deng, S. Kawi, Zeolite-based catalytic membrane reactors for thermo-catalytic conversion of CO_2, iScience 25 (2022) 105343.
[186] A. Rafiee, K.R. Khalilpour, D. Milani, M. Panahi, Trends in CO_2 conversion and utilization: a review from process systems perspective, J. Environ. Chem. Eng. 6 (2018) 5771–5794.
[187] H.B. Zhao, A.W. Li, J.H. Gu, G.X. Xiong, H. Brunner, A novel preparation method for porous noble metal/ceramic catalytic membranes, J. Mater. Sci. 34 (1999) 2987–2996.
[188] J. Lu, Q.Q. Chen, S.B. Chen, H. Jiang, Y.F. Liu, R.Z. Chen, Pd nanoparticles loaded on ceramic membranes by atomic layer deposition with enhanced catalytic properties, Ind. Eng. Chem. Res. 59 (2020) 19564–19573.
[189] G. Centi, R. Dittmeyer, S. Perathoner, M. Reif, Tubular inorganic catalytic membrane reactors: advantages and performance in multiphase hydrogenation reactions, Catal. Today 79–80 (2003) 139–149.
[190] M. Peng, Y. Liu, H. Jiang, R. Chen, W. Xing, Enhanced catalytic properties of Pd nanoparticles by their deposition on ZnO-coated ceramic membranes, RSC Adv. 6 (2016) 2087–2095.
[191] H. Jiang, X.X. Sun, Y. Du, R.Z. Chen, W.H. Xing, Catalytic activity of palladium nanoparticles immobilized on an amino-functionalized ceramic membrane support, Chin. J. Catal. 35 (2014) 1990–1996.
[192] D.M. Dotzauer, A. Abusaloua, S. Miachon, J. Dalmon, M.L. Bruening, Wet air oxidation with tubular ceramic membranes modified with polyelectrolyte/Pt nanoparticle films, Appl. Catal. B Environ. 91 (2009) 180–188.
[193] H.Y. Li, H. Jiang, R.Z. Chen, Y. Wang, W.H. Xing, Enhanced catalytic properties of palladium nanoparticles deposited on a silanized ceramic membrane support with a flow-through method, Ind. Eng. Chem. Res. 52 (2013) 14099–14106.
[194] R. Dittmeyer, V. Höllein, K. Daub, Membrane reactors for hydrogenation and dehydrogenation processes based on supported palladium, J. Mol. Catal. Chem. 173 (2001) 135–184.
[195] Y.H. Zhou, H.Q. Ye, R. Schomäcker, Selective hydrogenation of 1,5-cyclo-octa-diene over porous Pd/α-Al_2O_3 active membrane, Chin. J. Catal. 28 (2007) 715–719.
[196] S. Bhattacharjee, D.M. Dotzauer, M.L. Bruening, Selectivity as a function of nanoparticle size in the catalytic hydrogenation of unsaturated alcohols, J. Am. Chem. Soc. 131 (2009) 3601–3610.
[197] Y. Chen, S.Q. Fan, J.J. Chen, L. Deng, Z.Y. Xiao, Catalytic membrane nanoreactor with Cu-Ag_x bimetallic nanoparticles immobilized in membrane pores for enhanced catalytic performance, ACS Appl. Mater. Interfaces 14 (2022) 9106–9115.
[198] R. Brunet Espinosa, D. Rafieian, R.G.H. Lammertink, L. Lefferts, Carbon nano-fiber based membrane reactor for selective nitrite hydrogenation, Catal. Today 273 (2016) 50–61.
[199] H. Jiang, S.Q. Wang, Q.Q. Chen, Y. Du, R.Z. Chen, ZIF-derived Co/Zn bimetallic catalytic membrane with abundant CNTs for highly efficient reduction of p-Nitrophenol, Ind. Eng. Chem. Res. 61 (2022) 7862–7873.
[200] C. Iwakura, Y. Tsuchiyama, K. Higashiyama, E. Higuchi, H. Inoue, Successive hydrogenation and dechlorination systems using palladized ion exchange membranes, J. Electrochem. Soc. 151 (2004) D1.
[201] T. Sato, A. Takada, N. Itoh, Low-temperature hydrogenation of toluene by electrolysis of water with hydrogen permeable palladium membrane electrode, Chem. Lett. 46 (2017) 477–480.
[202] A. Huang, Y. Cao, R.S. Delima, T. Ji, R.P. Jansonius, N.J.J. Johnson, C. Hunt, J. He, A. Kurimoto, Z. Zhang, C.P. Berlinguette, Electrolysis can be used to resolve hydrogenation pathways at palladium surfaces in a membrane reactor, JACS Au 1 (2021) 336–343.



Dr. Jiuxuan Zhang received his PhD degree in chemical engineering and technology from Nanjing Tech University in 2021 under the supervision of Prof. Rizhi Chen. He then joined Nanjing Tech University as a postdoctor under the supervision of Prof. Yong Wang. His research mainly focuses on the design and fabrication of catalytic membranes for hydrogenation.

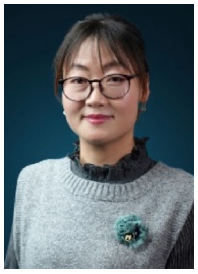

Dr. Yan Zhang obtained her Ph.D. degree in Industrial Catalysis from Dalian Institute of Chemical Physics in 2014. After that, she joined the Center of Functional Membrane and Hydrogen Energy Technology, Qingdao Institute of Bioenergy and Bioprocess Technology, Chinese Academy of Sciences (QIBEBT, CAS). She is currently a professor in QIBEBT, CAS. Her research focuses on membrane separation and catalysis.



Dr. Xuefeng Zhu is a professor of physical chemistry and chemical engineering at Dalian Institute of Chemical Physics (DICP), Chinese Academy of Science (CAS). He received his PhD degree (2007) from DICP. He has coauthored more than 130 peer-reviewed scientific papers and holds more than 20 patents. His research interests focus on mixed conducting ceramic membranes and solid oxide cells for process intensification and energy conversion.



Dr. Aisheng Huang is a professor of inorganic chemistry at East China Normal University. He received his PhD degree (2005) from Dalian Institute of Chemical Physics, CAS. His research focuses on the development and applications of molecular sieve membranes and catalytic membrane reactor. He has published more than 120 SCI-indexed papers, and holds more than 20 patents.



Heqing Jiang obtained his PhD degree in Physical Chemistry at Leibniz University of Hannover (Germany). After his post-doctoral stay at Max Planck Institute for Coal Research (Germany), he joined in 2013 as a full professor at Qingdao Institute of Bioenergy and Bioprocess Technology, Chinese Academy of Science (QIBEBT, CAS). His main research interest focuses on the multifunctional membranes and their applications in separation and catalysis.



Dr. Rizhi Chen is a professor of Chemical Engineering at Nanjing Tech University. He received his PhD degree (2004) from Nanjing Tech University. He was recipient of Chang Jiang Scholars Program. His research focuses on the development and applications of membrane reactors. He has published more than 150 SCI-indexed papers, and holds more than 30 patents.